(18) DOE

(19) (12)

WT-524 (EX)
EXTRACTED VERSION

(6)

OPERATION SNAPPER

Project 2.3
Neutron Flux Measurements.

(9) Rept. for Apr-Jun 52.

Nevada Proving Grounds
April-June, 1952

(12) 65

NOTICE

This is an extract of **WT-524, Operation SNAPPER, Neutron Flux Measurements,** which remains classified **Secret/Restricted Data** as of this date.

(15) DNA001-79-C-0455

Extract version prepared for:
Director
DEFENSE NUCLEAR AGENCY
Washington, D. C. 20305

(11) 1 February 1980

Approved for public release; distribution unlimited.

REPORT DOCUMENTATION PAGE

READ INSTRUCTIONS BEFORE COMPLETING FORM

1. REPORT NUMBER: WT-524 (EX)
2. GOVT ACCESSION NO.: AD-A995
3. RECIPIENT'S CATALOG NUMBER: 033

4. TITLE (and Subtitle): Operation SNAPPER
Project 2.3-Neutron Flux Measurements

5. TYPE OF REPORT & PERIOD COVERED:

6. PERFORMING ORG. REPORT NUMBER:

7. AUTHOR(s):

8. CONTRACT OR GRANT NUMBER(s):

9. PERFORMING ORGANIZATION NAME AND ADDRESS:

10. PROGRAM ELEMENT, PROJECT, TASK AREA & WORK UNIT NUMBERS:

11. CONTROLLING OFFICE NAME AND ADDRESS:

12. REPORT DATE: April-June 1952

13. NUMBER OF PAGES: 53

14. MONITORING AGENCY NAME & ADDRESS (if different from Controlling Office):

15. SECURITY CLASS. (of this report): Unclassified

15a. DECLASSIFICATION/DOWNGRADING SCHEDULE:

16. DISTRIBUTION STATEMENT (of this Report)

Approved for public release; unlimited distribution.

17. DISTRIBUTION STATEMENT (of the abstract entered in Block 20, if different from Report)

18. SUPPLEMENTARY NOTES

This report has had the classified information removed and has been republished in unclassified form for public release. This work was performed by the General Electric Company-TEMPO under contract DNA001-79-C-0455 with the close cooperation of the Classification Management Division of the Defense Nuclear Agency.

19. KEY WORDS (Continue on reverse side if necessary and identify by block number)

Atmospheric Nuclear Tests
Nevada Test Site
Operation SNAPPER
Neutron Flux
Neutron Dosimetry Techniques
Biological Studies
Neutron Detectors
Fission Threshold Detectors

20. ABSTRACT (Continue on reverse side if necessary and identify by block number)

The objective of Project 2.3 was to provide measurements of neutron flux for the interpretation of biological studies and the study of neutron dosimetry techniques. It was the goal of the project to cover as thoroughly as possible the neutron spectrum encountered in the detonation of the nuclear fission bombs. In this endeavor Project 2.3 was to augment the work of the AEC Laboratories and try experimental techniques on a field trial basis.

FOREWORD

This report has had classified material removed in order to make the information available on an unclassified, open publication basis, to any interested parties. This effort to declassify this report has been accomplished specifically to support the Department of Defense Nuclear Test Personnel Review (NTPR) Program. The objective is to facilitate studies of the low levels of radiation received by some individuals during the atmospheric nuclear test program by making as much information as possible available to all interested parties.

The material which has been deleted is all currently classified as Restricted Data or Formerly Restricted Data under the provision of the Atomic Energy Act of 1954, (as amended) or is National Security Information.

This report has been reproduced directly from available copies of the original material. The locations from which material has been deleted is generally obvious by the spacings and "holes" in the text. Thus the context of the material deleted is identified to assist the reader in the determination of whether the deleted information is germane to his study.

It is the belief of the individuals who have participated in preparing this report by deleting the classified material and of the Defense Nuclear Agency that the report accurately portrays the contents of the original and that the deleted material is of little or no significance to studies into the amounts or types of radiation received by any individuals during the atmospheric nuclear test program.

The study of neutron flux and energy distribution from the "weapons effects" point of view can yield information significant for the interpretation of biological studies, and for the study of neutron dosimetry techniques. Project 2.3 was established for this purpose in order to augment the work of the AEC laboratories, and to provide an opportunity to introduce experimental techniques on a field trial basis. In general the procedures that have been established by LASL at previous tests were followed. Sulphur was used as a threshold detector for fast neutrons, and gold was used as a detector for slow neutrons. Tantalum was used on a trial basis in order to study it in comparison with gold as a slow neutron detector. Nuclear track emulsions were exposed in lead shields on an experimental basis in an attempt to study the energy spectrum in the 1 Mev to 4 Mev region. A number of fission threshold detectors were tried both with foils to catch the fission products for subsequent counting in a flow counter and with nuclear track emulsions to catch the fission products for microscope counting.

The fluxes of "sulphur" and "gold" neutrons in the range intervals of biological interest can be characterized by the absorption coefficient or e-fold distance and the intercept at the range = 0 axis. This data is summarized in the following table:

	Sulphur		Gold	
Shot	e-fold dx	O=intercept	e-fold dx	O=intercept
3			190 yds.	2.8×10^{16}
4			200 yds.	7.4×10^{16}
8			190 yds.	2.8×10^{16}

The proton recoil emulsions were exposed at ranges calculated to bracket the optimum range for the measurement. A compromise must be made between neutron intensity and gamma ray fog. Adequate exposures were obtained at Shots 4 and 8. The fission threshold detectors are most promising. However, because of inherent difficulties in their use and because of the short time available for their preparation, fluxes versus range were not obtained. Flux measurements at specific ranges of particular interest were made, however.

Sulphur and gold are dependable as neutron detectors. Extensive use of these materials in the past has eliminated most of the technical

PP. 1 & 2 deleted

difficulties. Nuclear track emulsions suffer from the fact that they must be shielded against gamma rays, thus introducing neutron scattering material and complicating the analysis. Fission threshold detectors show promise, but require that the foil catchers be counted within hours of exposure. If nuclear track emulsions are used to catch fission fragments, special provision must be made to prevent excessive blackening of the emulsion by the natural radioactivity of the detector materials.

It is recommended that further effort be extended to find dependable threshold detectors and to develop laboratory techniques for their use. Nuclear track emulsion techniques are promising, but considerable laboratory study will be required to prepare them for field use.

Fission detectors were shown feasible for neutron dosimetry in effects tests. Effects of photo fission were small at ranges of about 1000 yards. Uranium-238, with a threshold 1 Mev lower than $S^{32}(n,p)$, detected several times the neutron flux measured by S^{32}; this is in agreement with the expected neutron spectrum. The attenuation of fast neutrons in lead appears more nearly linear than exponential.

OBJECTIVES

The objective of Project 2.3 was to provide measurements of neutron flux for the interpretation of biological studies and the study of neutron dosimetry techniques. It was the goal of the project to cover as thoroughly as possible the neutron spectrum encountered in the detonation of the nuclear fission bombs. In this endeavor Project 2.3 was to augment the work of the AEC Laboratories and try experimental techniques on a field trial basis.

With the aforementioned goal in mind, gold was used as a detector for neutrons in the thermal region. Tantalum was used in conjunction with gold to provide a detector less sensitive than gold in order that higher thermal fluxes might be measured. In high fluxes it has been necessary to wait until the induced activity in gold has gone through several half lives before counting could be undertaken. Tantalum, being only 1/100 as sensitive, can eliminate the time delay.

Sulphur, having an effective threshold at 3 Mev, was used as the detector for fast neutrons for this energy and above.

Nuclear track emulsions were used in an experimental attempt to determine the neutron flux and its spectrum from 1 Mev on up. This technique makes use of the recoil proton spectrum produced in emulsions by the neutron spectrum.

The fission detectors were used to provide flux measurements in the region between thermal energies and the 3 Mev energies detected by sulphur. This too, is an experimental technique and was used in an attempt to make flux measurements in the neutron energy spectrum in a region of great biological significance, which previously has not been covered.

p. 6 deleted

PREFACE

Because of the distinct differences in techniques, the report of the work of Project 2.3 is divided into three major parts.

ACKNOWLEDGEMENTS

Project 2.3 duplicated in some respects the work of Los Alamos Scientific Laboratory in neutron measurements at the SNAPPER tests. Counting arrangements and samples were intercalibrated by means of special calibration samples counted by both laboratories. For Shot 3, duplicate installations were made for gold and sulphur samples and the data were compared in order to check the calibration. The authors wish to thank the J division of LASL for the aid given to this project both in the calibration and the field operation phases. In particular, thanks are due to William E. Ogle, Clyde L. Cowan, Jr. and Martin Warren for permission to use the experimental line established for their diagnostic work.

The authors also wish to express their appreciation to Maurice M. Shapiro and co-workers for their support in the analysis, and their discussions on the interpretation of the proton recoil data.

p. 8 deleted

CONTENTS

ABSTRACT 3

OBJECTIVES 5

PREFACE 7

ACKNOWLEDGMENTS 7

ILLUSTRATIONS 11

TABLES 11

PART I GOLD, SULPHUR AND TANTALUM DETECTORS 13

CHAPTER 1 GOLD AS A SLOW NEUTRON DETECTOR 13

1.1 Background 13
1.2 Calibration 15
1.2.1 Standard Source 15
1.2.2 Counting Method 15
1.3 Field Exposure Containers 16
1.4 Sample Locations 16
1.4.1 Shot 3 16
1.4.2 Shot 4 16
1.4.3 Shot 8 19
1.5 Data and Calculations 19
1.5.1 Counting Loss Correction 19
1.5.2 Cadmium Correction Factor 21
1.5.3 Gold Calibration Number 21
1.5.4 Sample Calculation 22
1.6 Experimental Data 22
1.6.1 Shot 3 23
1.6.2 Shot 4 23
1.6.3 Shot 8 23
1.7 Conclusions 26
1.8 Recommendations 26

CHAPTER 2 TANTALUM AS A SLOW NEUTRON DETECTOR 27

2.1 Background 27
2.1.1 Tantalum Reactions 27
2.1.2 Tantalum Shielding 27
2.2 Calibration 28
2.3 Field Exposure Containers and Locations 28
2.4 Data and Calculations 28
2.5 Conclusions 28
2.6 Recommendations 28

CHAPTER 3 SULPHUR AS A NEUTRON THRESHOLD DETECTOR 32

3.1 Background 32
3.2 Calibration 32
3.3 Field Exposure Containers 33
3.4 Data and Calculations 33
3.5 Conclusions 33

PART II PROTON RECOILS IN NUCLEAR TRACK EMULSIONS 38

CHAPTER 4 USE OF NUCLEAR TRACK EMULSIONS AS NEUTRON DETECTORS . . . 38

4.1 Background 38
4.2 Theory 40
4.3 Experimental Method 40
4.3.1 Scanning Method 41
4.4 Data 42
4.5 Discussion and Conclusion 42
4.6 Recommendations 42

PART III FISSION THRESHOLD DETECTORS 51

CHAPTER 5 FISSION THRESHOLD DETECTORS 51

5.1 Background 51
5.1.1 Catcher Method 51
5.1.2 Foil Method 52
5.1.3 Nuclear Emulsion Method 52
5.1.4 Energy Response of Fission Detectors 54
5.2 Instrumentation 54
5.2.1 Catcher Method 54
5.2.2 Foil Method 54
5.2.3 Nuclear Emulsion Method 55
5.3 Operations 56
5.4 Results 61
5.5 Conclusions 63
5.6 Recommendations 63

ILLUSTRATIONS

1.1 Au and Cd Cross-section Curves 14
1.2 Au and S Sample Holders 17
1.3 Gold Data Summary 24
1.4 Biological Gold Data 25

2.1 Cd and Ta Cross-section Curves 29
2.2 Shot 4 Data 30

3.1 Sulphur Data Summary 34

4.1 Proton Recoil Distribution 43
4.2 Angular Distribution for Plate 1 44
4.3 Angular Distribution for Plate 2 45
4.4 Spectrum Distribution for Plate 1 46
4.5 Spectrum Distribution for Plate 2 47
4.6 Spectrum Distribution for Plates 1 and 2 48
4.7 Theoretical Prompt Fission Neutron Energy Spectrum 49
4.8 Neutron Energy Spectrum 50

5.1 Relative Response of Fission Detectors and Sulphur to Moderated Fast Neutron Fission Flux 53
5.2 Neutron Attenuation in Lead 60
5.3 Relative Fast Neutron Attenuation 62

TABLES

1.1 Shot 3 Gold Data 18
1.2 Shot 4 Gold Data 18
1.3 Shot 8 Gold Data 20
1.4 Summary Gold Data 20

2.1 Shot 4 - Tantalum Data 31

3.1 Shot 3 Sulphur Data 35
3.2 Shot 4 Sulphur Data 35
3.3 Shot 8 Sulphur Data 36
3.4 Summary Sulphur Data 37

5.1 Data Shots 4 and 8 57

p. 12 deleted

PART I

GOLD, SULPHUR AND TANTALUM DETECTORS

CHAPTER 1

GOLD AS A SLOW NEUTRON DETECTOR

1.1 BACKGROUND

The measurement of thermal neutron flux by use of materials in which a convenient radioactivity is induced by neutron capture has become a widely accepted technique. At SANDSTONE [1] the Los Alamos Scientific Laboratory used arsenic as a detector for thermal neutrons. Although the activity induced in a contaminant (Sb^{123}) hampered the analysis, it was possible to separate the activity resulting from the reaction $As^{75}(n,\gamma)As^{76}$ (26.8 hour decay period) from the activity resulting from the reaction $As^{75}(n,2n)As^{74}$ (17 day decay period). This latter activity is also produced by gamma rays $As^{75}(\gamma,n)As^{74}$. The threshold for the (n,2n) reaction is about 10.3 Mev. Thus arsenic serves as a detector for both thermal neutrons and neutrons above 10.3 Mev. Unfortunately the activation cross section for arsenic is large and it becomes very "hot". Since arsenic is difficult to handle, the induced activities excessively high, and the analysis tedious, gold was used as a slow neutron detector at RANGER and at GREENHOUSE [2,2a]. Gold is monoisotopic. Its cross section for the (n,2n) reaction is small. The interesting reaction in this application is $Au^{197}(n,\gamma)Au^{198}$. The Au^{198} decays by emission of a 0.97 Mev beta particle and a 0.411 Mev gamma ray in cascade to stable Hg^{198}. The half life of the activity is 2.69 days [3]. The cross section for gold exhibits a resonance to epithermal neutrons in the region of 5 ev. In order to use gold as a detector of slow neutrons it is necessary to make use of the cadmium difference technique. Cross sections for Cd and Au are shown in Fig. 1.1. Gold samples are exposed with and without cadmium shields. The difference in the activity of the two samples is then proportional

---

1/ SANDSTONE Scientific Director's Report, Vol. 18, Annex 4, Part 1 and Addendum thereto, dated 1948.

2/ GREENHOUSE Neutron Measurements (Internal preliminary report of Los Alamos Scientific Laboratory LAB-J-2102).

2a/ Neutron Measurements at Operation Ranger, LASL Report LAB-J-2095 (No. 2 and 2a by Ogle, Cowan, et al.)

3/ National Bureau of Standards Bulletin 499.

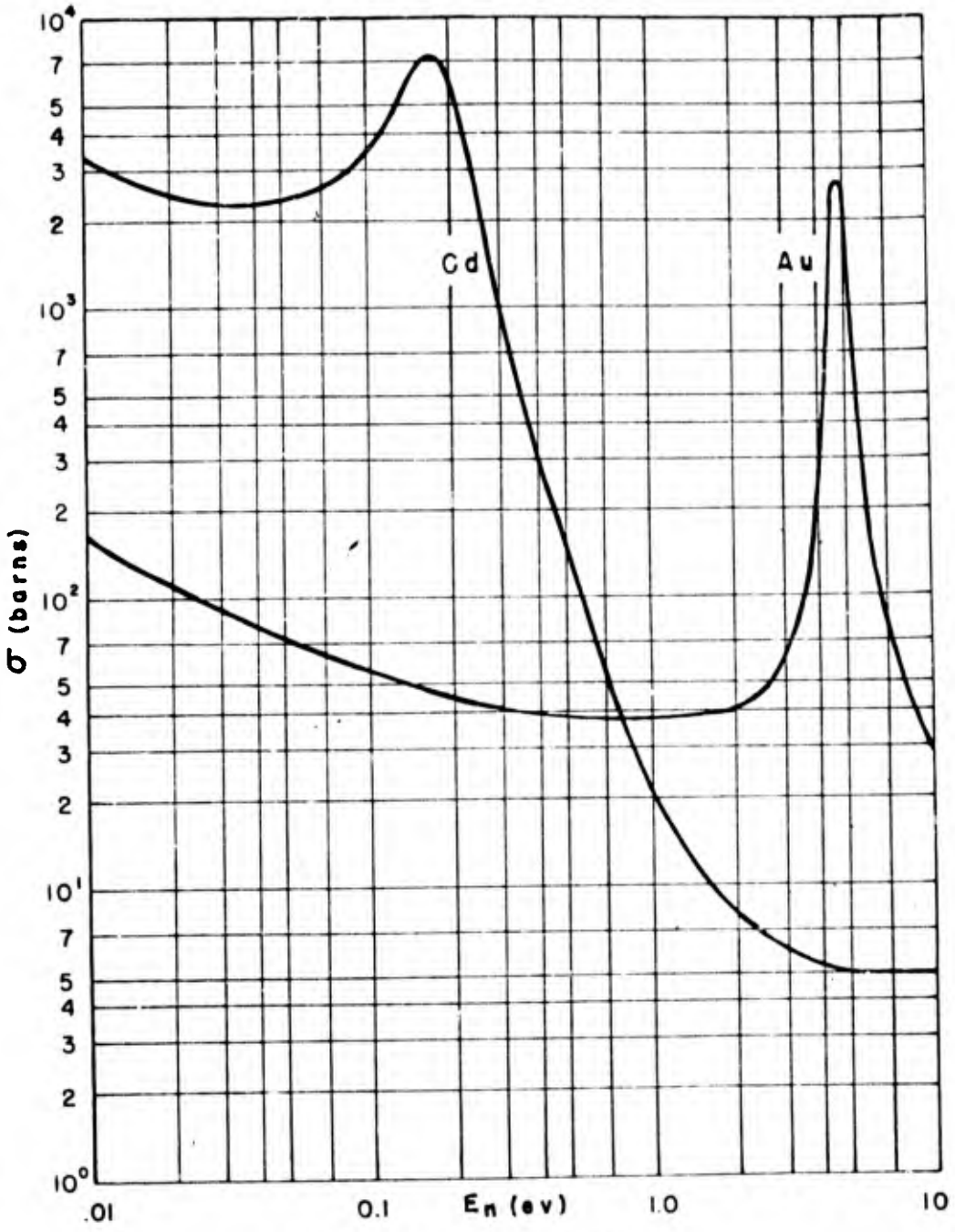

Fig. 1.1 σ_t for Cd and Au

to the flux of neutrons below the "cadmium cutoff." Although the "difference" will include some activity resulting from neutrons somewhat above thermal energies, it is taken as a measure of thermal flux.

1.2 CALIBRATION

The calibration of gold for use as a slow neutron detector has been done by the Los Alamos Scientific Laboratory using a standard neutron source available there. In order to make use of this calibration, samples of gold exposed under standard conditions were counted several times in the counters at NRL and LASL over a period of several half-lives. This permitted the calculation of a calibration number for use with the NRL geometry and counting arrangement. For the sake of clarity and completeness, a description of the general features of the calibration technique will be repeated. A more complete discussion of the calibration method will undoubtedly appear in the forthcoming LASL report on the GREENHOUSE neutron measurements.

1.2.1 Standard Source

The standard source used by LASL to calibrate gold is the Standard Graphite Pile containing the standard radium-beryllium source Number 44. The absolute value for the flux from source Number 44 is known to be $5.90 \times 10^6 \pm 5$ per cent neutrons per second as of 1 December 1944. (This source was calibrated in standard piles by A. C. Graves and R. Walker. A comparison source was also calibrated at Argonne) [2]. The distribution of thermal neutrons in the pile as a function of distance from the source is known with an uncertainty of about 1 per cent [2]. The position chosen for the calibration of the gold foils was one for which the cadmium ratio indicated the presence of an appreciable percentage of higher energy neutrons in order to simulate the actual conditions in the radiation field of an atomic weapon where the neutron flux is expected to consist of a degraded fission spectrum. In computing the thermal flux at the chosen position, allowance is made for the growth factor (the increase in alpha particle emission as the radium approaches equilibrium with its descendants) and for the drain or self shadowing factor [4]. The probable error in this particular calibration is estimated as 6 per cent.

1.2.2 Counting Method

The gold calibration made by LASL used 1/2" diameter discs 0.010" thick. In order to simplify intercalibration the gold samples for Project 2.3 were prepared to these same dimensions. By counting the gold samples which had been given a standard exposure at LASL in

---

[4] W. Bothe, Zeits. F. Phys. 120, 437 (1943).

both the NRL counters and the LASL counters, an intercalibration factor was determined. This calibration was checked by means of duplicate samples installed in the LASL test line at Shot 3. The gold foils were counted in commercial preflush methane flow counters. No counts of less than 10,000 were taken in order that the counting statistics might be uniform. Each sample was counted several times over a period of several half lives to assure that the activity was that of Au^{198}. The performance of the scaling equipment was checked regularly with a Bi^{210} standard source which was used because the beta particle energy (1.17 Mev) is near that of Au(.97 Mev).

1.3 FIELD EXPOSURE CONTAINERS

Cowan and co-workers at LASL have shown that the attenuation of thermal neutron and epithermal neutron flux within the detection range of the gold detectors is negligible [2] for the 0.25" thick holders used at GREENHOUSE and RANGER. The sample holders used for Project 2.3 were similar to the LASL holders except for minor details. The steel container used for the gold samples is shown in Fig. 1.2. The web on the back plate of the container permits clamping it to the recovery cable or to the steel stakes used at ranges greater than 1000 yds.

1.4 SAMPLE LOCATIONS

Project 2.3 participated in Shots 3, 4, and 8. The LASL Group assisted the project by permitting 2.3 to use their existing instrument line.

1.4.1 Shot 3

Gold sample locations are given in Table 1.1.

1.4.2 Shot 4

Gold sample locations are given in Table 1.2. Sample holders No. 8, 9, and 10 were placed in the Project 4.3 line at the station known as George. For each test one station in the Project 4.3 line was chosen for instrumentation as complete as facilities would permit. In addition to the other detectors placed at this station as noted in later sections of this report, gold samples were exposed in several thicknesses of lead in order to estimate the attenuation of the slow neutrons in the shields that were required to protect the experimental animals and in some cases the detectors themselves from the effects of the gamma ray flux. Holder No. 8 was placed without lead shielding. Holder No. 9 was placed inside the lead hemisphere used for the Project 4.3 animals (7" of lead shield). Holder No. 10 was placed inside a special pure lead spherical shield having 2" wall thickness.

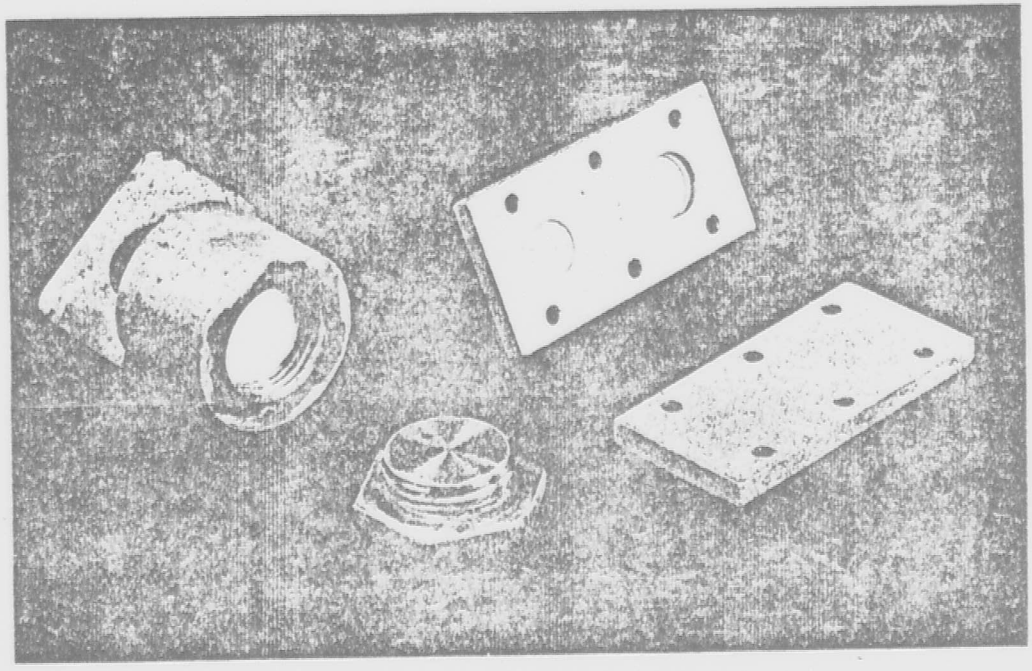

Fig. 1.2 Au and S Sample Holders

TABLE I.1

Shot 3 Gold Data

Station #	Slant Range Yards	Holder #	Sample #	nvt ± 10%	nvt x R
182	1172	40	S-79, S-80	6.84×10^{10}	8.01×10^{13}
184	1227	62	S-123, S-124	4.53×10^{10}	5.56×10^{13}
186	1313	53	S-105, S-106	2.815×10^{10}	3.69×10^{13}
188	1422	90	S-179, S-180	1.83×10^{10}	2.60×10^{13}
190	1547	97	S-193, S-194	8.28×10^{9}	1.28×10^{13}

TABLE I.2

Shot 4 Gold Data

Station #	Slant Range Yards	Holder #	Sample #	nvt ± 10%	nvt x R
182	426	1	A-1, A-2	7.34×10^{13}	3.13×10^{16}
184	562	2	A-3, A-4	1.56×10^{13}	8.56×10^{15}
186	732	3	A-5, A-6	3.07×10^{12}	2.25×10^{15}
188	912	4	A-7, A-8	8.40×10^{11}	7.65×10^{14}
190	1099	5	A-9, A-10	2.67×10^{11}	2.35×10^{14}
195	1581	6	A-11, A-12	1.434×10^{10}	2.345×10^{13}
200	2072	7	A-13, A-14	1.07×10^{9}	2.21×10^{12}
George(0")*	1027	8	A-15, A-16	3.48×10^{11}	3.57×10^{14}
George(7")	1027	9	A-17, A-18	2.75×10^{11}	2.82×10^{14}
George (2")	1027	10	A-19, A-20	3.38×10^{11}	3.47×10^{14}

*Thickness of lead shield.

1.4.3 Shot 8

Gold samples were placed as shown in Table 1.3. Sample holders No. 24 through 27 were placed in the Project 4.3 line at the station known as Easy. Station Easy was the station chosen for complete instrumentation for Shot 8. Holder No. 24 was placed without lead shielding. Holder No. 25 was placed inside the lead hemisphere having 7" wall thickness. Holder No. 26 was placed inside a pure lead sphere having 4" wall thickness. Holder No. 27 was placed inside a pure lead sphere having 2" wall thickness.

1.5 DATA AND CALCULATIONS

The samples were collected at the earliest possible moment after exposure and returned to the laboratory quonset at Camp Mercury for counting. The Evans Signal Laboratory provided the radiac equipment AN/MDQ-1(XE-3) for use as a field counting laboratory. The counting equipment that had been calibrated at NRL was installed in this van for operation at Mercury. Except for the very hot samples, counting was begun on the day of the exposure. When conditions permitted rapid recovery, it was possible to begin counting within four hours after the exposure time.

1.5.1 Counting Loss Corrections

For short half life detectors, it is obvious that early counting is necessary. Regardless of the half life, however, it is desirable to get complete data as quickly as possible. Thus some development of high speed counting equipment was undertaken. Using available commercial equipment it was found that the counting loss resulting from the resolving time of the discriminator and scaling strips limited the speed to rates under 1000 per second. By making minor modifications in selected commercial equipment it was possible to observe counting rates up to 25,000 per second with counting loss corrections of 20 per cent or less. The equipment finally chosen for use in the field consisted of pre-flush methane flow counters (Radiation Counter Lab Mk12 Mod 2), linear amplifiers (Atomic Instrument Co. Model 1213) and fast scalers (Atomic Instrument Co. Model 1030 with 1 microsecond scaling strips installed). The overall effective resolving time of this system turned out to be approx. 5 microseconds. The high voltage power supply (4200 volts) was provided by the Higgenbotham circuit 5/ which provided better regulation than required. The resolving time mentioned above was measured by means of the multiple source method. Small discs of tantalum (1/4" diameter) were exposed in groups to a wide range of neutron fluxes. For the counting loss determination an exposure group was chosen so that the counting rate of an individual of the group would

---

5/ Rev. Sci. Instr. 22, No. 6, 429(L), 1951. W. A. Higgenbotham.

TABLE I.3

Shot 8 Gold Data

Station #	Slant Range Yards	Holder #	Sample #	nvt ±10%	nvt x R
2-102	224	11	A-21, A-22	1.93×10^{14}	4.32×10^{16}
2-104	412	12	A-23, A-24	2.18×10^{13}	8.96×10^{15}
2-106	608	13	A-25, A-26	5.00×10^{12}	3.04×10^{15}
2-108	806	14	A-27, A-28	6.62×10^{11}	5.34×10^{14}
2-110	1005	15	A-29, A-30	1.63×10^{11}	1.635×10^{14}
2-111	1104	16	A-31, A-32	9.60×10^{10}	1.06×10^{14}
2-112	1204	17	A-33, A-34	5.25×10^{10}	6.32×10^{13}
2-114	1403	18	A-35, A-36	1.42×10^{10}	2.0×10^{13}
2-116	1603	19	A-37, A-38	3.86×10^{9}	6.19×10^{12}
2-120	2004	20	A-39, A-40	4.37×10^{8}	8.75×10^{11}
Easy*(0")	1105	24	A-47, A-48	8.72×10^{10}	9.09×10^{13}
Easy (7")	1105	25	A-49, A-50	1.37×10^{11}	1.515×10^{14}
Easy (4")	1105	26	A-51, A-52	9.86×10^{10}	1.09×10^{14}
Easy (2")	1105	27	A-53, A-54	1.12×10^{11}	1.24×10^{14}

*Thickness of lead shield.

TABLE I.4

Summary Gold Data

Shot	Zero Intercept	e-fold Distance
3	2.8×10^{16} (nvt x R)	190 yds
4	7.4×10^{16} (nvt x R)	200 yds
8	2.8×10^{16} (nvt x R)	190 yds

require only a small correction. The sums of individual counting rates were compared to the counting rates of the appropriate groups of samples. Using the formula

$$n_t = \frac{n_o}{1 - n_o t}$$

the resolving time t was computed by successive approximation using the value of t to correct the individual counting rates for the next calculation of the resolving time. As a test of the accuracy of the counting rate corrections, and to estimate the highest counting rates that could be accepted, initial counting rates were calculated from several counts taken on a gold sample. The initial counting rates calculated from points taken after many half lives agreed within the 1 per cent statistics with the initial counting rates calculated from counts taken earlier in the decay for counting rates requiring up to 25 per cent correction. No counting data requiring more than a 20 per cent correction were used for the final calculations. The gold samples were counted in aluminum planchets designed to hold the sample in standard position. The gold samples were sufficiently thick that corrections for back scattering from the aluminum were not necessary. Because of the directional effect that has been observed in previous tests [3] the gold samples were counted both front and back and the activity of the sample was taken as the average of the front and back surface counts (this counting method is implicit in the calibration process).

1.5.2 Cadmium Correction Factor

As previously noted, gold exhibits a resonance in the region of 5 ev. The cadmium difference technique is used to eliminate the activity arising from this resonance. The cadmium cross section falls rapidly above 0.2 ev, but at higher neutron energies it flattens out, so that a considerable number of epithermal neutrons is absorbed. Since the difference between the activity of a shielded and an unshielded sample is the measure of the slow neutron flux, the absorption of epithermal neutrons by the cadmium introduces a substantial error in the difference even though the correction itself is small. The correction for the cadmium (LASL data [2]) is $1.025 \pm .015$. The activity of the cadmium shielded sample is corrected by this factor before the cadmium difference is taken.

1.5.3 Gold Calibration Number

In paragraph 1.2.2 it was stated that the calibration was derived by counting samples exposed to known flux at LASL. This calibration number was used in the reduction of the data from Shot 3 so as to compare the final results with results from an identical installation made by LASL. Table 1.1 contains the results of this test. The e-fold distance and zero intercept supplied by LASL agree with the same figures

for the NRL data within the precision of the measurement, (LASL 200 yds and 2.75×10^{16}; NRL 200 yds $\pm$ 5 per cent and $2.80 \times 10^{16} \pm 5$ per cent). The calibration numbers for LASL and NRL are respectively 7.74×10^5 neutrons cm^{-2} per count per minute, and 8.09×10^5 neutrons cm^{-2} per count per minute.

1.5.4 Sample Calculation

The several counts taken on each sample were extrapolated back to the exposure time to determine the Initial Counting Rate (ICR) by means of

$$ICR = CR_t \exp\left[\lambda(t-t_o)\right]$$

where Cr_t is the counting rate at the time t
λ is the decay constant for the Au^{198} activity
t_o is the time of exposure.

From the published half life of Au^{198} the decay constant is 1.788×10^{-4} per minute [3]. The slow neutron flux is then given by

$$nvt = K(ICR_{bare} - 1.025 \times ICR_{Cd}) \text{ neutrons per } cm^2$$

where ICR_{bare} is the initial counting rate for the unshielded gold sample, ICR_{Cd} is the initial counting rate for the cadmium shielded gold sample and K is the calibration number = 8.09×10^5 neutrons per cm^2 per count per minute. The initial counting rates used for the calculation of the flux were the averages of initial counting rates calculated for the several counts made on each sample.

1.6 EXPERIMENTAL DATA

The experimental data consisting of counting rates as a function of time were converted to flux data as shown above. Following the convenient procedure established in previous work, the final data are presented in tabular form with estimates of precision and in graphical form. The studies made at RANGER with arsenic and subsequently at GREENHOUSE with gold have shown that the attenuation of the slow neutrons with increasing range is not exponential. The curve is more nearly exponential if the flux times range is plotted vs range. If flux times range squared is plotted vs range the departure from a straight line occurs in the region of biological interest (i.e., at the low intensity end of the curve). In the graphical presentation of the data that follows, nvt x R is plotted vs R. For ranges beyond several hundred yards nvt x R was very nearly exponential. The slow neutron flux at small ranges was substantially greater than the extrapolated exponential line indicates. It appears that two processes were involved. Since the gold detectors are sensitive only to slow neutrons, there are

two classes of neutrons capable of activating the detector; the neutrons born fast that were degraded in the atmosphere after making a large angle collision at a large distance from the source, and the neutrons which were born slow within the device so that it becomes a point source of slow neutrons. Neutrons born fast provided the 1/R attenuation at great ranges, and the combination of degraded fast and slow neutrons gave the increased intensity at small ranges. It will be noted that the attenuation of fast neutrons was exponential thus supporting the notion that the fast flux undergoes only small angle scattering before detection, and that large angle scattering degrades the energy below the detection threshold before the diffusion effect can be observed in detectors with thresholds in the Mev range.

1.6.1 Shot 3

Five samples were placed in the field for shot 3. The height of burst prevented placing samples closer than approximately 1100 yards. (See Table 1.1). The e-fold distance, from this data, is approximately 190 yds. The range = 0 intercept of a line through the data at this slope is 2.8×10^{16} nvt x R. The data are summarized in Table 1.1 and the graph Fig. 1.3.

1.6.2 Shot 4

Seven samples were placed in the LASL line, three samples were used to help instrument one station in the Biomedical experimental line for Project 4.3. Location of samples is given in Table 1.2. The e-fold distance is about 200 yds. The range = 0 intercept is 6.6×10^{16} nvt x R. The data taken in the Biomed line are shown with the data from the LASL line both in the Table 1.2 and in the graph Fig. 1.3. Figure 1.4 presents the data from station George on an expanded scale permitting the differences observed for different thicknesses of lead to be plotted. The estimated error in the measurements is also shown.

1.6.3 Shot 8

Ten samples were placed in the LASL line, four samples were used to instrument one station in the Biomed line. Location of samples is given in Table 1.3. The e-fold distance is again about 200 yds. The range = 0 intercept is 2.8×10^{16} nvt x R. Data are displayed in Table 1.3. Figure 1.3 is a plot of the slow neutron data. Figure 1.4 is an expanded version of the range interval near the Easy station showing the data taken in different thicknesses of lead. It is obvious that the effect of lead shielding on the intensity of thermal flux is small compared to the precision of the measurement since the points are scattered both above and below the values for the unshielded samples.

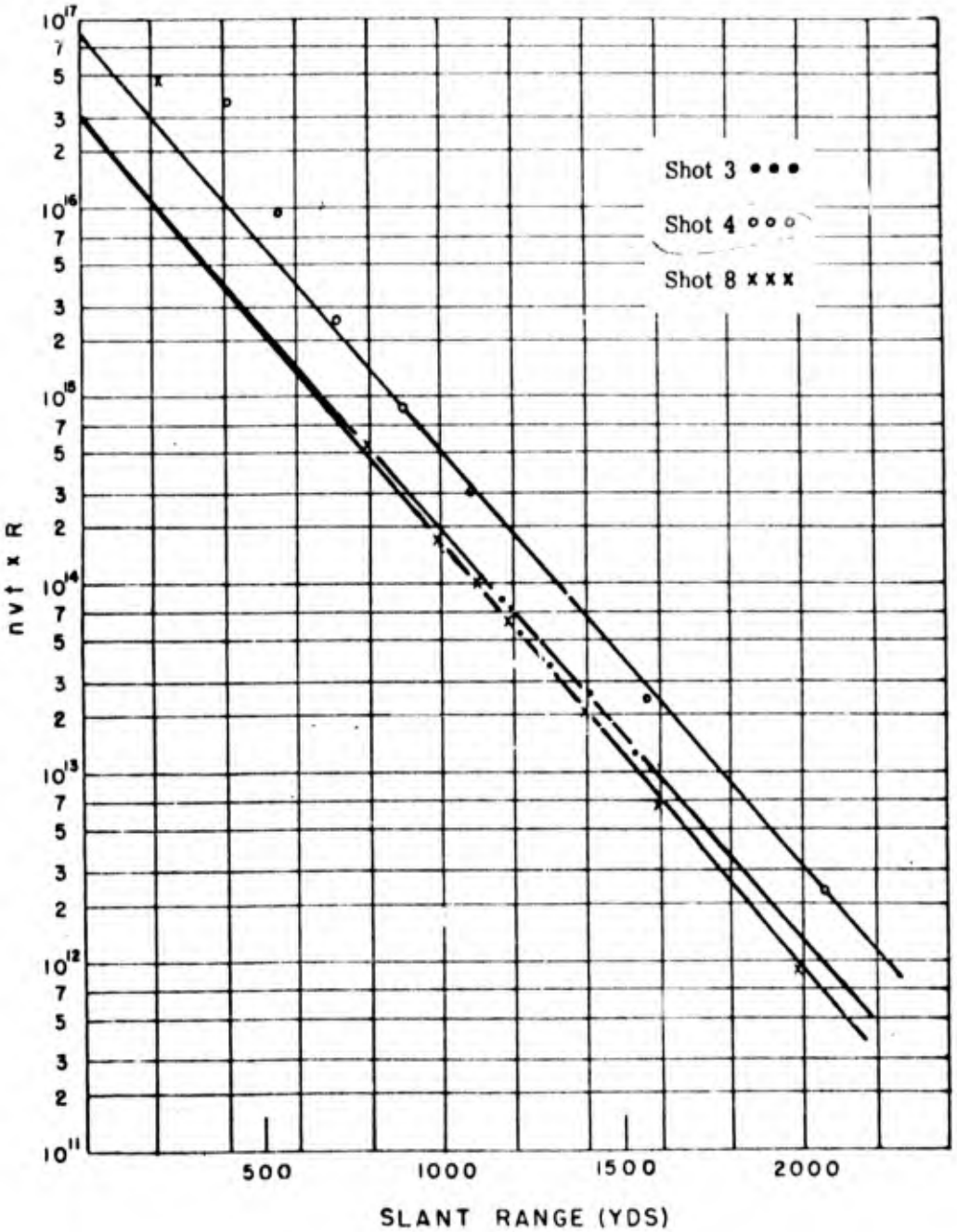

Fig. 1.3 Gold Data Summary

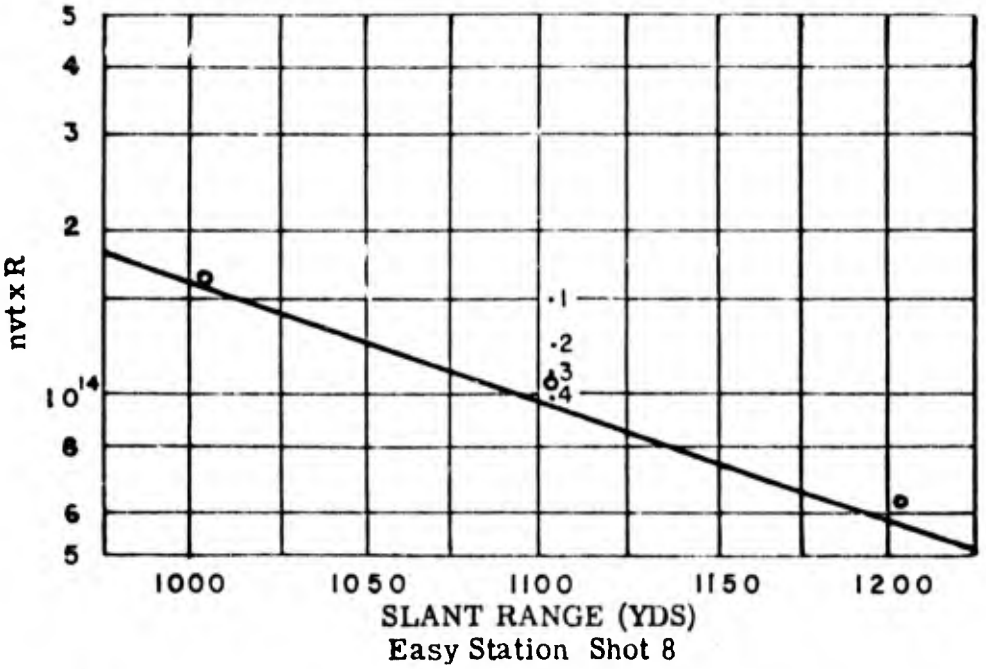

Easy Station Shot 8

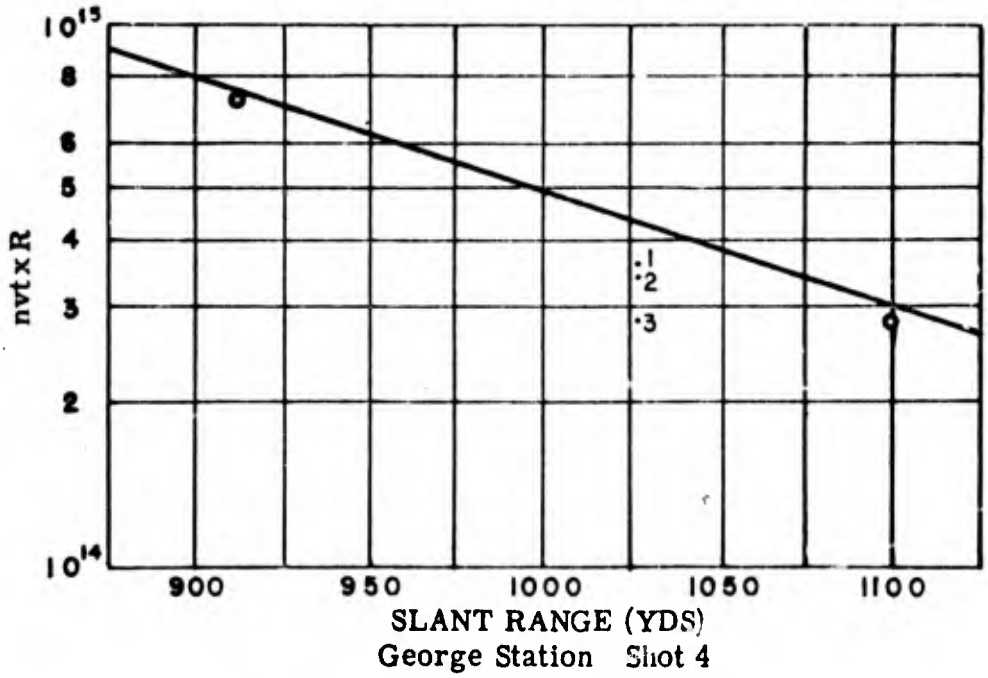

George Station Shot 4

Fig. 1.4 Biological Gold Data

1.7 CONCLUSIONS

No attempt has been made to relate thermal neutron flux to the KT equivalent of the particular devices tested. The work of the LASL has already shown that the neutron flux does not scale, but is some function of many characteristics of the structure besides the KT equivalent. Figure 1.3 presents a superposition of the three sets of data for gold. This is given merely for convenience in comparing the fluxes from the three devices tested. Apparently, the numbers of high energy neutrons present were not great enough to activate the 5.6 day half life resulting from the reaction $Au^{197}(n,2n)Au^{196}$. This activity may present difficulties if gold is used as a detector of slow neutrons from a thermo-nuclear device from which large fluxes of high energy neutrons are expected. Since the plot of the slow neutron flux is very nearly exponential when nvt times R is plotted vs. R (except at small ranges where thermals born in the device add to the flux of degraded neutrons) it is possible to characterize the flux vs. range plot by a slope and a Y axis intercept. From this information a graph of the thermal neutron flux for ranges greater than say 700 yds can be constructed by passing a line through the range = 0 intercept at the slope corresponding to the e-fold distance. Table 1.4 is a summary of the e-fold distances and the zero intercepts for the three events studied.

1.8 RECOMMENDATIONS

Gold is a sensitive detector for slow neutrons at ranges of biological interest. At ranges where gold becomes too active, tantalum can be used. The convenient half life, large cross section, and absence of interfering activities recommends gold as a detector.

CHAPTER 2

TANTALUM AS A SLOW NEUTRON DETECTOR

2.1 BACKGROUND

In the course of the preparation for the work of Project 2.3, pile activated tantalum provided convenient sources of high activity for use in measuring counting losses. Because of its smaller cross section for slow neutrons and its greater half life, the activity for a given slow neutron flux is in the order 0.005 times the activity of a similar gold sample. The lower sensitivity of tantalum presented the possibility of using it for the measurement of slow neutrons in the ranges for which gold samples become too hot to count for many half lives.

2.1.1 Tantalum Reactions

The interesting reaction in tantalum results from $Ta^{181}(n,\gamma)Ta^{182}$. Tantalum[182] has a complicated decay scheme characterized by two half lives. There are many gamma rays and several beta particles. Observable half lives are 117 days and 16.4 minutes [3]. The cross section associated with the 117 day activity is 21 barns. The cross section for the 16.4 minute activity is 0.034 barns [3]. Because of the relatively small cross section, and the fact that in a few hours it dies away by a factor of 1000, the 16.4 minute activity does not interfere. The γ,n and n,2n reactions with tantalum lead to an activity of Ta^{180} with a half life of 8.0 hours. This activity was not observed.

2.1.2 Tantalum Shielding

Since tantalum has a series of resonances beginning at about 3.5 ev it is necessary to use the cadmium difference technique as used with gold [6]. Unfortunately, time was not available to determine the cadmium correction factor for tantalum. The data here presented were calculated using the cadmium correction determined for gold samples. Figure 2.1 presents the cross section curves for cadmium [1] and tantalum [6]. Figure 2.2 presents the tantalum curve plotted with the gold curve. The calibration number for tantalum was determined in this case by equating the range = 0 intercepts. On this plot the curves have different slopes because of the error implicit in using the gold cadmium correction for the tantalum cadmium difference.

---

[6] Havens et al Phys. Rev. 71, 165 (1947).
[1] Rainwater et al Phys. Rev. 71, 65 (1947).

Comparison of the slopes of the normalized curves indicates that the cadmium correction should be considerably larger than the 2 1/2 per cent used for gold.

2.2 CALIBRATION

Tantalum was used only for Shots 4 and 8. No specific calibration was made for tantalum. The activity induced in the tantalum has not been followed long enough to be sure that there are no interfering activities. The data obtained from tantalum are compared with those from gold, and the calibration number for tantalum is expressed in terms of the calibration for gold, thus any error in the gold calibration is carried over into the tantalum calibration.

2.3 FIELD EXPOSURE CONTAINERS AND LOCATIONS

Tantalum was exposed in the gold holders. The method used for shielding was identical with that used for gold. The location of samples is given in Table 2.1.

2.4 DATA AND CALCULATIONS

The data shown in Table 2.1 were calculated in a manner similar to the methods used for gold. The tantalum data for Shot 8 are not graphed, since these data were used only at close range.

2.5 CONCLUSIONS

Although it is too early to conclude that tantalum makes a good detector for slow neutrons, the appearance of the data taken to date seems to indicate that it will provide a good supplement to gold for the intensity range that leads to high activity in gold. The activity of tantalum will be followed at this laboratory until it is sure that there are no interfering activities.

2.6 RECOMMENDATIONS

An independent calibration of tantalum should be made before it can be depended on as a slow neutron detector.

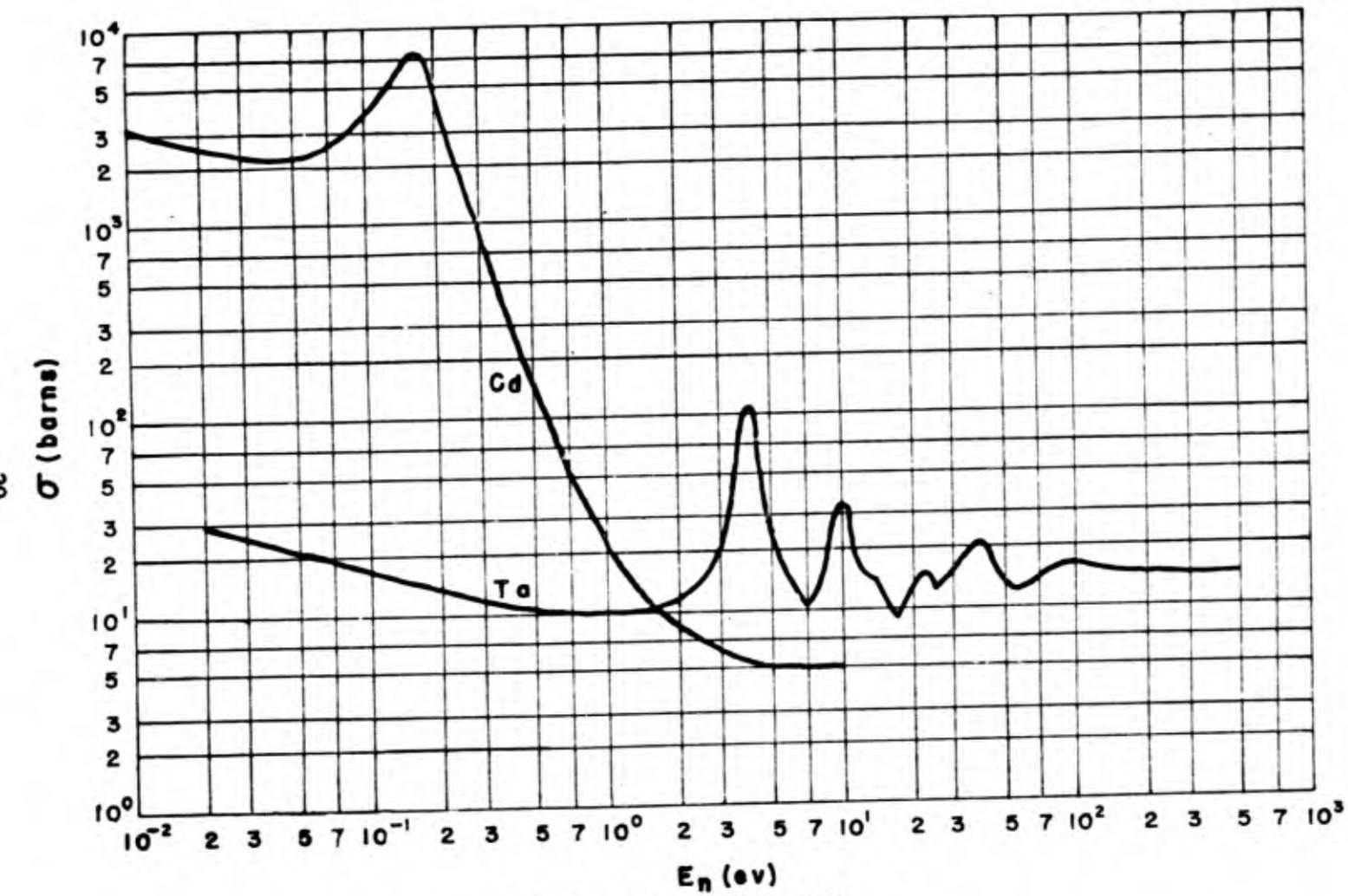

Fig. 2.1 σ_t for Cd and Ta

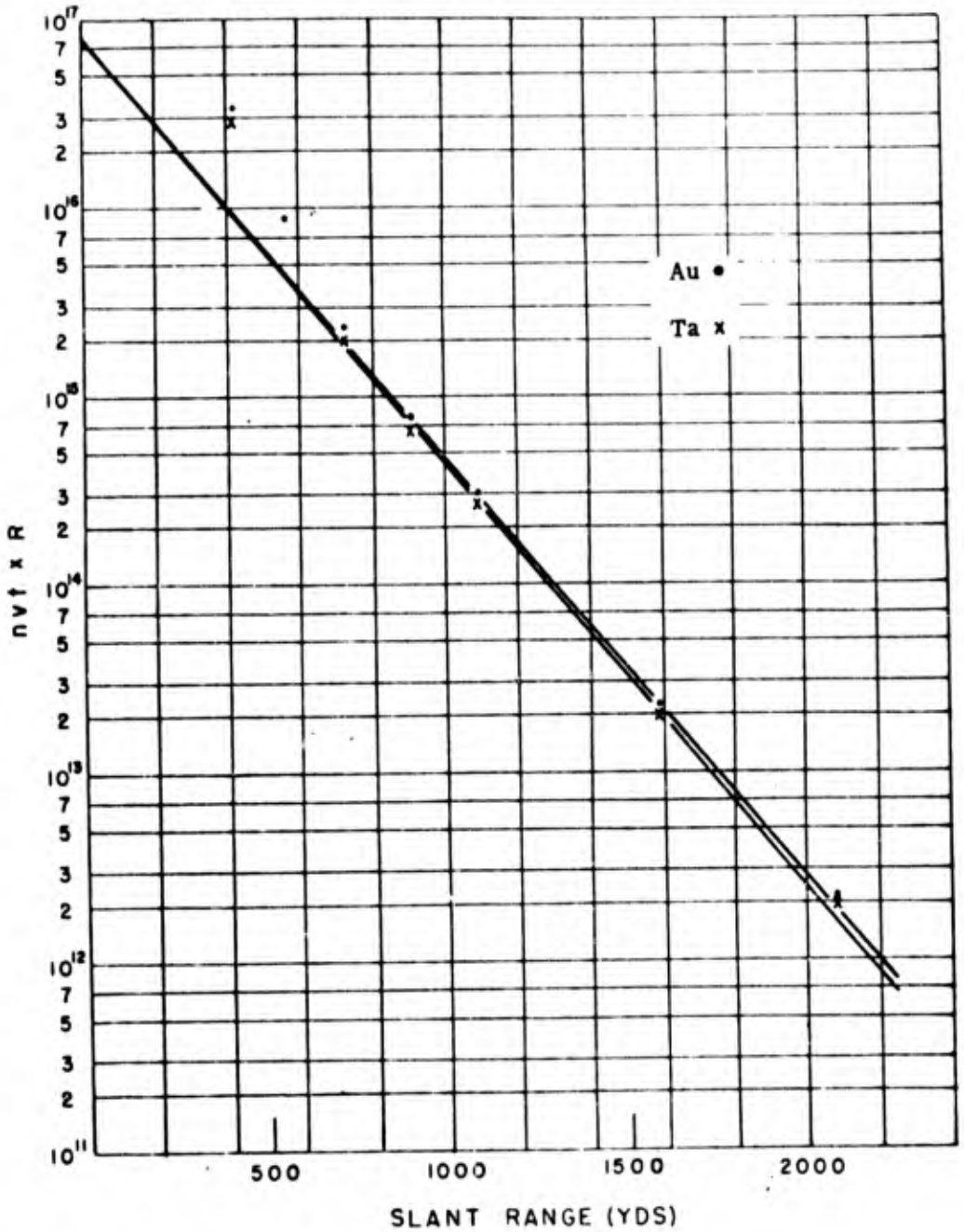

Fig. 2.2 Shot 4 Data

TABLE 2.I
Shot 4 - Tantalum Data

Station #	Slant Range Yards	Holder #	Sample #	Cd-DiffxR ± 10%	nvt x R
182	426	1-C	C-1, C-2	1.205×10^{8}	2.73×10^{16}
186	732	3-C	C-5, C-6	8.71×10^{6}	1.97×10^{15}
188	912	4-C	C-7, C-8	2.90×10^{6}	6.56×10^{14}
190	1099	5-C	C-9, C-10	1.14×10^{6}	2.58×10^{14}
195	1581	6-C	C-11, C-12	8.70×10^{4}	1.80×10^{13}
200	2072	7-C	C-13, C-14	9.13×10^{3}	2.06×10^{12}
2-102	224	C-11	C-17, C-18	1.03×10^{8}	2.34×10^{16}
2-104	412	C-21	C-19, C-20	4.53×10^{7}	1.03×10^{16}
2-106	608	C-31	C-21, C-22	9.12×10^{6}	2.07×10^{15}
2-108	806	C-41	C-23, C-24	2.66×10^{6}	6.03×10^{14}
2-110	1005	C-51	C-25, C-26	5.03×10^{5}	1.14×10^{14}

CHAPTER 3

SULPHUR AS A NEUTRON THRESHOLD DETECTOR

3.1 BACKGROUND

Sulphur has been widely used as a detector for fast neutrons. It was first used for measurements of nuclear devices at TRINITY. It has been used subsequently at Bikini 8/, SANDSTONE 1/, and GREENHOUSE 2/. The reaction of interest is $S^{32}(n,p)P^{32}$. Phosphorous^{32} is a pure beta emitter. The possible interfering activities are not present to a measurable extent. The cross section for this reaction has been measured in some detail by Klema 9/, Linnenberger 1/, and Dodds 2/. The effective threshold is taken to be 3.0 Mev and it is assumed that the cross section is approximately flat above this value. Phosphorous ^{32} decays by emission of a 1.7 Mev beta particle with a half life of 14.59 days 10/. In contrast with other (n,p) threshold detectors, the cross section for this reaction for sulphur rises rapidly above the energetic threshold. The presence of a resonance in the region of 2.4 Mev produces this effect, otherwise the cross section would have a slow increase above the energetic threshold corresponding to the penetration of the potential barrier by the escaping proton.

3.2 CALIBRATION

Klema 9/ calibrated sulphur as a threshold detector for the TRINITY test. More recent calibrations have been made at LASL appropriate to the counting systems proposed for GREENHOUSE 2/. The more recent work at LASL has been directed toward the use of pressed pellets of sulphur instead of the cast cylinders employed at TRINITY and SANDSTONE. The calibration number used by Project 2.3 was obtained from LASL data supplied with the gold calibration data. Sublimed sulphur was exposed to the neutrons from the D,T reaction on a Cockroft-Walton set. The average energy of the neutrons in the exposure position for the sulphur (90° from the beam) was 14.14 Mev. The number of neutrons emitted was measured by counting the alphas emitted in the reaction. The sublimed sulphur was then pressed into a 2 gram pellet of 1 inch diameter. The calibration number was determined by counting in both the LASL and NRL counting geometries. The calibration number for the NRL arrangement is $K = 3.05 \times 10^{7}$ neutrons per cm^2 per count per minute.

8/ Los Alamos Scientific Laboratory Report - LAMS 447
9/ Klema, LASL Report LA-515
10/ W. K. Sinclair, A. F. Holloway, Nature 167, 365 (1951)

3.3 FIELD EXPOSURE CONTAINERS

The sublimed sulphur was exposed at SNAPPER in steel cups containing about 6 grams of material (see Fig. 1.2). Except for the sample that melted, 2 grams of the exposed sulphur were weighed out and transferred to a pellet die. Ten thousand psi produces a dense smooth pellet for counting in the methane flow counter geometry. The sample that melted at the test was remelted at about 130°C and poured into a mold for counting. Tests made with pile activated sulphur gave the same counting rate (within statistics) both for pellet and the molded samples.

3.4 DATA AND CALCULATIONS

The data for the sulphur measurements for Shots 3, 4 and 8 are given in Tables 3.1, 3.2 and 3.3 respectively. Because of its small cross section, sulphur is not a suitable detector for integrated fluxes less than about 10^8 neutrons per cm^2 unless special provisions are made to count a large sample. The 1 inch discs used for TUMBLER-SNAPPER provided readable measurements down to about 5×10^8 neutrons per cm^2. The graph, Fig. 3.1, presents a plot of sulphur neutron flux x R^2 vs range for Shots 3, 4, and 8 respectively. Also plotted on the graph of Fig. 3.1 are the activities of several sulphur samples exposed in various thicknesses of lead. When the logarithms of these activities are plotted against the lead thickness, it is evident that the absorption of sulphur activating neutrons is not exponential. It is certain that the process of degradation of fast neutrons in spherical shields is complex, and that one would not expect that the absorption could be characterized by a simple absorption coefficient. The spectrum is expected to be a monotonically decreasing function in the region above 3 Mev [redacted]. The absorption coefficient (or total cross section) vs energy for neutrons in lead is nearly constant above 3.0 Mev. Thus possible explanations of the absorption curves would look to the geometry of the shield and to the spectrum shape in the 3 Mev region.

3.5 CONCLUSIONS

As noted in the chapter on gold, it was not the purpose of Project 2.3 to make measurements for diagnostic purposes. Hence the conclusions for the sulphur are the data themselves and a few comments on the utility of sulphur as a fast neutron detector. Sulphur serves adequately and inexpensively as a detector of fluxes greater than 10^8 neutrons per cm^2. The techniques for its use are well established. Figure 3.1 is a composite showing for comparison sulphur neutron flux x R^2 for the three tests. Intercept and slope data are summarized in Table 3.4.

Pages 34 thru 37 Deleted

PART II

PROTON RECOILS IN NUCLEAR TRACK EMULSIONS

CHAPTER 4

USE OF NUCLEAR TRACK EMULSIONS AS NEUTRON DETECTORS

4.1 BACKGROUND

Nuclear track emulsions have found widespread application in measurements of neutron flux and energy spectrum. Several advantages are immediately evident; - a) simplicity of the detector, and b) integrating effect, i.e. the time integrated flux is recorded. A number of techniques for specific applications have been developed. Rosen [2] used a collimator to measure the prompt neutron spectrum by means of recording the recoil protons emitted from a radiator outside the emulsion. To extend the energy range of the method, various thicknesses of absorber were used in front of the emulsions. Such methods using good geometry permit direct interpretation of the proton recoil spectrum observed. For observations of isotropic neutron flux, Reines [11] has proposed a method of analysis for calculating the neutron spectrum from the proton recoil spectrum. Evans [12] has developed a scanning technique that permits the use of medium thick emulsions to determine the spectrum over a limited energy range. Evans' scanning technique requires that two plates be exposed to the isotropic flux. These plates are arranged so that the planes of the emulsions are perpendicular. The criterion for accepting a track is that it lie within certain limiting angles. These angles are chosen so that the correction for shrinkage in the emulsion is not great, and so that tracks in the total solid angle are counted and thus anisotropic fluxes can also be measured. This "two-plate" method can be used to study the neutron spectrum over an energy range limited by the thickness of the emulsion.

4.2 THEORY

In order to interpret the energy spectrum of the proton recoils observed in a photographic emulsion, a relation between the incident neutron spectrum and the recoil proton spectrum must be derived. Since the scattering of neutrons considered in the center of mass system is spherically symetrical (this is a reasonably good assumption for n,p

---

11/ F. Reines, Phys. Rev. 74, 1565 (1948)
12/ J. E. Evans, Los Alamos Publication LAMS 1312 (1951)

scattering for neutron energies below about 10 Mev.), the relation between the spectra can be derived by means of elementary considerations. Thus the differential cross section for scattering into a solid angle $d\Omega$ in the center of mass system is proportional to $d\Omega$. The neutron and proton play interchangeable roles, so that this is also the cross section for proton recoils. The element of solid angle between θ and $\theta + d\theta$ is $2\pi \sin\theta d\theta = 2\pi d(\cos\theta)$. All values of $\cos\theta$ are equally likely. The ratio E/E_n is a linear function of $\cos\theta$ (or $\cos 2\theta$ in the lab system), hence the probability that a proton will recoil with the energy lying between E and E+dE is just dE/E_n where E_n is the incident neutron energy. The spectrum distribution for protons recoiling from neutrons of energy E_n is constant for E_p lying between 0 and E_n, and zero for E_p greater than E_n. Let P(E) be the proton recoil spectrum amplitude in protons per Mev per cm^3. The number of recoil protons produced by a group of neutrons having energy E is EdP. The total number of recoils produced by the distribution of neutrons is then

$$N_p = \int_0^{E_{max}} E \frac{dP(E)}{dE} dE$$

where the limits of integration refer to the neutron energy. The number of recoil protons can also be computed from the neutron spectrum. Let N(E) be the neutron flux in neutrons per Mev per cm^2 as a function of the neutron energy E. Then the number of recoil protons per cm^3 due to neutrons of energy E is $\rho N(E)\sigma(E)dE$, and the total number of protons is

$$N_p = \int_0^{E_{max}} \rho N(E)\sigma(E)dE$$

where ρ is the number of hydrogen atoms per cm^3 and $\sigma(E)$ is the neutron proton scattering cross section per cm^2. By equating the two integrals and differentiating both sides we have the expression relating the proton recoil spectrum with the neutron spectrum that produces them;

$$N(E) = \frac{E}{\rho \sigma(E)} \frac{dP(E)}{dE}$$

If the energy dependence of the proton spectrum has the form of $1/E^n$, this relation says that the neutron spectrum will have the same form. The prompt neutron spectrum resulting from fission has been studied by B. E. Watt [13]. By assuming a Maxwellian distribution for the fission

13/ B. E. Watt, Los Alamos Report LA-718

neutrons ($E^{\frac{1}{2}}e^{-E/Q}$ in the center of mass system), an expression for the energy spectrum of the neutrons is derived. To simplify the analysis one average group of fission fragments was assumed. Constants were chosen for best representation of the data. The resulting formula is:

$$N(E) = \text{Const.} \times \sinh(2E)^{\frac{1}{2}}\, e^{-E}$$

Somewhat better fit to the experimental data was obtained when the distribution was calculated for two groups of fission fragments, but for the purposes of this report, the goodness of fit for the expression above is better than the precision of this experiment.

4.3 EXPERIMENTAL METHOD

Following the method developed by Evans and Reines (loc cit), the films were prepared for exposure in aluminum holders arranged to hold two films so that the emulsions were perpendicular to each other. Ilford E1 emulsions 100 microns thick were used. These were preferred to the C2 emulsions because the sensitivity to gamma rays for the E1 emulsions proved to be about one-fourth the sensitivity of the C2 emulsions. At the time that the lead shields were designed, the gamma-ray flux expected was uncertain by a factor of about 10. On the basis of such preliminary estimates of the gamma-ray flux, the lead shields were designed for about 0.1 per cent transmission of the gamma rays. The shields were cast from high purity lead (99.998 per cent) in the shape of a cylinder 12" in diameter by 15" long. The high purity was required in order to minimize neutron capture gamma rays in antimony. The film holders were inserted in a 1½" diameter hole in the shield which was closed with a lead plug. The minimum thickness of the lead surrounding the plates was 5.13". The plates were placed so that the surface of the emulsion made an angle of 45 degrees with the horizontal. The lead shields were placed in the field at locations calculated to bracket the optimum range for readable recoil tracks. The gamma-ray intensity at the ranges chosen for Shot 4 were approximately 3500r, 400r and 100r. For Shot 8 the lead shields were placed at ranges of 1100, 1600 and 2000 yards. After exposure the films were recovered along with the activation samples and were sent by courier plane to NRL for processing.

4.3.1 Scanning Method

The limitation on scanning time prevented the application of the Evans scanning procedure. In its stead, a set of plates from Shot 8 was analyzed according to a scanning schedule recommended by M. M. Shapiro and his co-workers. The criterion for an acceptable track is that it lie within plus or minus 10° of the surface plane of the emulsion. Range measurements were made for all such tracks. Enough tracks were measured on each plate to give reasonable statistics (500 tracks per plate were counted and measured). From these data,

angular distributions were plotted in order to consider the directional effects expected in the fast neutron flux. The thickness of the lead shield was such that less than 15 per cent of the incident neutrons reach the photographic plate without scattering. Only 1 or 2 per cent of the incident flux could penetrate the total thickness of the shield without scattering (these estimates are based on an assumed cross section of approximately 5 barns in the region from 1 to 5 Mev). Because of the thickness of the lead shield, it was expected that the anisotropy of the incident flux would not show in the angular distributions. This proved to be the case. However, it is possible to determine a line perpendicular to the incident flux. Since long proton recoil tracks normal to the incident flux could only arise from multiply scattered neutrons there should be a minimum in the angular distribution for the direction normal to the incident flux. This minimum was observed. Histograms showing the number of proton recoils per Mev were also plotted. A measure of the hardness of the neutron spectrum was made by plotting the average track length per unit solid angle versus angle. When the lower energy tracks were plotted in this fashion, the isotropy of the flux at the emulsion is evident. If the less frequent long tracks are included in the plot, the angular distribution becomes quite rough. No significance should be attributed to this other than to comment that the statistics for the long tracks as a function of angle are very poor.

4.4 DATA

The histograms, Fig. 1a, b, and c, present the number of tracks per Mev as a function of proton energy (converted from the range energy relation for Ilford C1 emulsions). Figure 1a and 1b show the distribution for Plates 1 and 2 separately. Figure 1c is the combined histogram for both plates. The graphs, Fig. 1.2 and 1.3, present the angular distribution of the proton recoil tracks. For the angular distribution, the number of acceptable tracks in each 20 degrees in azimuth lying within plus or minus 10 degrees of the surface of the emulsion is plotted versus azimuth. The distribution is more uniform if the tracks less than 60 microns are plotted. The tracks of range greater than 60 microns were few, and their effect on the distribution is to accentuate the roughness due to statistical uncertainty. On the same graphs the average track length per unit solid angle is plotted versus angle to indicate the hardness of the spectrum. These distributions were plotted to show that the distribution is sensibly the same in each plate, and to justify the combination of the data from the two plates. Figures 1.4 and 1.5 present the spectrum distribution for the proton recoils observed in the two plates. Figure 1.6 is the distribution for the recoils in both plates. The range at which the plates were exposed was 2000 yards. For this great a path length, the absorption of neutrons at the nitrogen resonances should be observable. However, the statistical uncertainty of the points in the region of the resonance is too great. Thus the energy resolution is not adequate to

show the absorption.

4.5 DISCUSSION AND CONCLUSIONS

The work of B. E. Watt [13] and others indicates that the prompt neutron spectrum from thermal fission is well fitted by a function $e^{-E}\sinh(2E)^{\frac{1}{2}}$. If it is assumed that the fast neutron spectrum at the 2000-yard range can be approximated by this same function, then the activity of the sulphur threshold detectors should be proportional to the integral of the flux above 3 Mev. Using the tabulated values of the normalized integral of the spectrum function above as given in the GREENHOUSE preliminary report, the spectrum amplitude at 3 Mev can be obtained. Using the sulphur data from Part I of this report, the amplitude at 3 Mev is 1.29×10^8 neutrons per cm^2 per Mev. Figure 1.7 is the normalized spectrum function as given by Watt. Figure 1.8 is a construction of the hypothetical spectrum through the point indicated by the sulphur activity using the spectrum function above. The sulphur point is indicated by an arrow. The scattered points shown on this graph are the points calculated from the proton recoil data. They are plotted to the same energy scale, but to an arbitrary ordinate scale in order to show the slope of the spectrum as calculated from proton recoils in comparison with the slope of the prompt neutron spectrum from thermal fission. The straight line is drawn to a slope of minus 7. On the basis of the proton recoil data, one may conclude that the energy degradation of the fast neutrons in passing through the atmosphere (and through lead shields) is such that this steep energy dependence results. In the absence of data, in the region below 1 or 2 Mev it is not possible to estimate the neutron intensities in this region. The proton recoil data do not provide information down to energies low enough to permit an estimate of the energy for which the intensity is maximum. In order to make full use of the threshold detector technique some knowledge of the spectrum shape is required. For biomedical purposes the spectrum shape should be measured in a "poor geometry" arrangement, since the intensity of radiation scattered into the detector may be a significant portion of the total intensity.

4.6 RECOMMENDATIONS

The proton recoil method for the measurement of neutron spectra is most useful when used in a "good geometry" or collimated arrangement. The uncollimated arrangement used in this experiment presents rather great difficulties in scanning and in interpretation of the results. A theoretical treatment of the diffusion problem applied to the fission neutron spectrum is required in order that best use can be made of the data that can be taken with threshold detectors. Further effort toward the development of threshold detectors having thresholds in the region below 1 Mev is recommended.

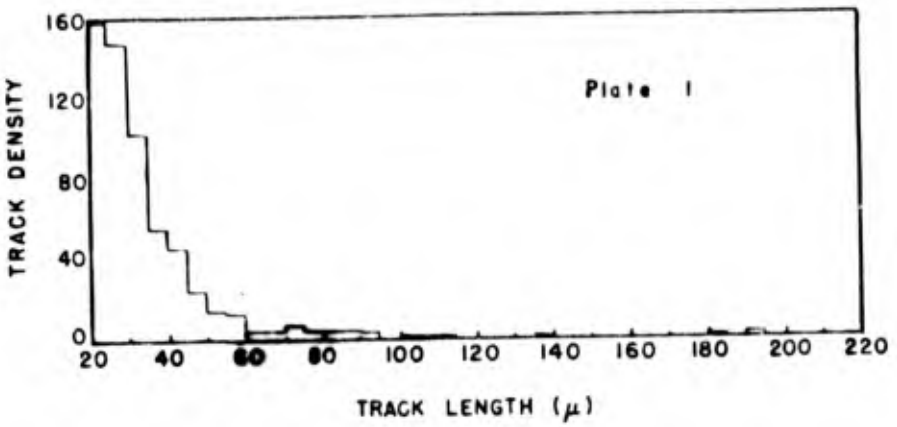

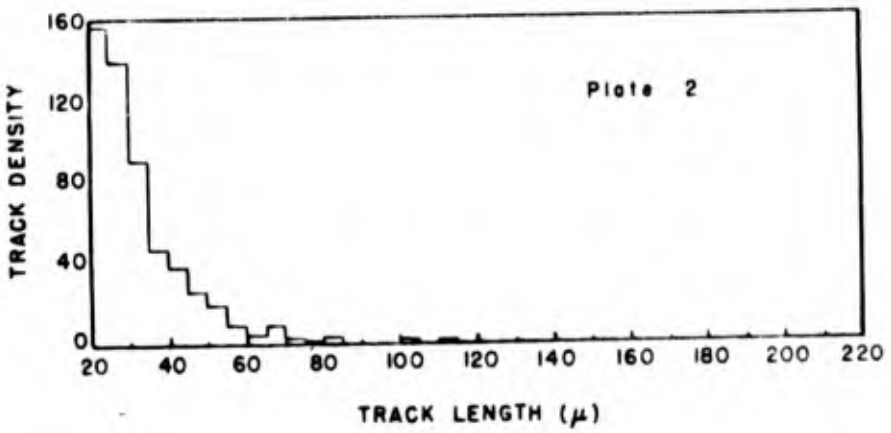

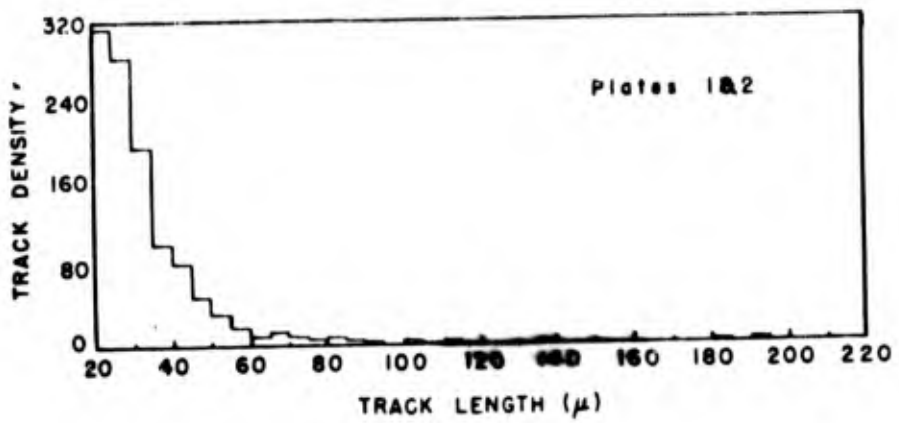

Fig. 4.1 Proton Recoil Distribution

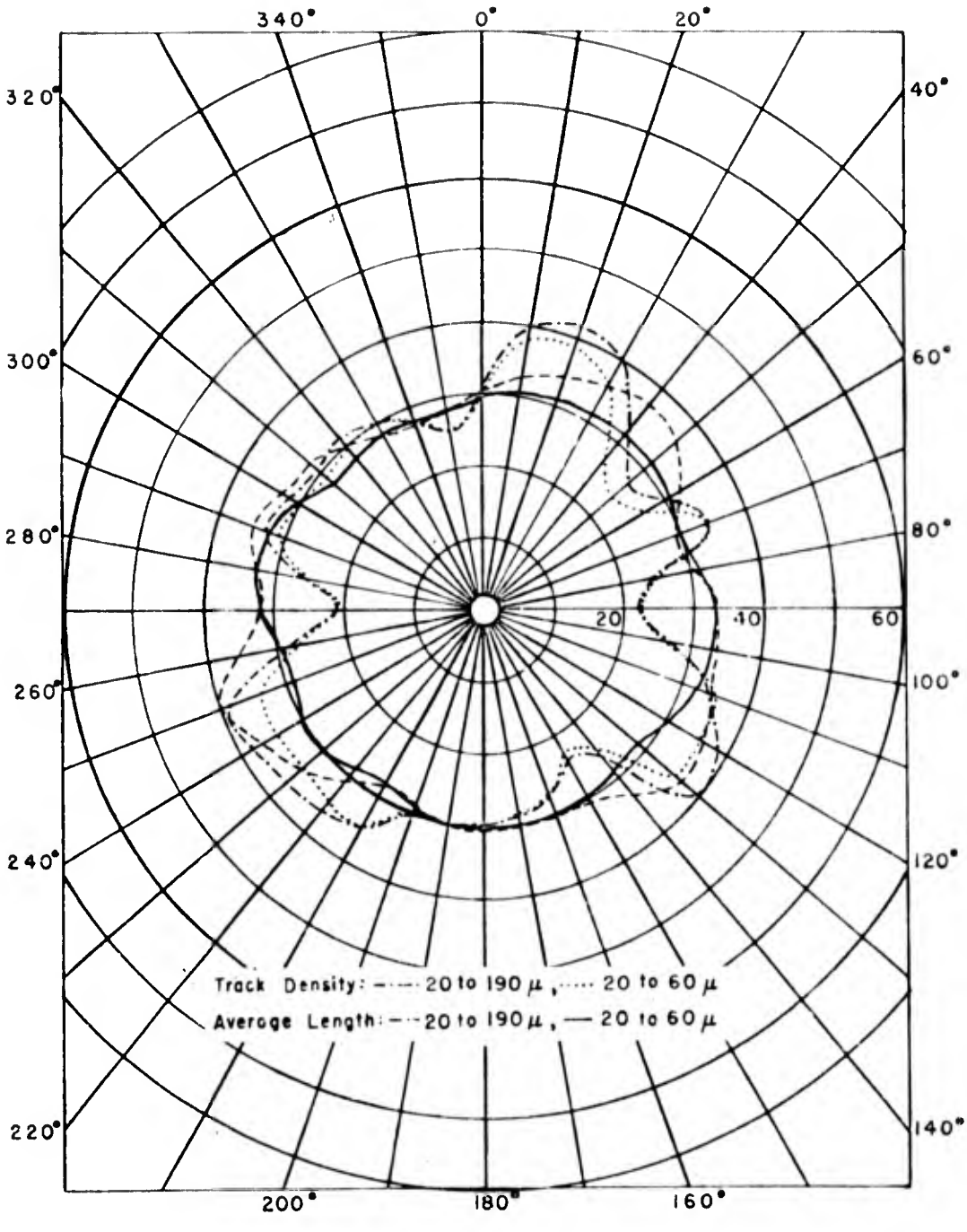

Fig. 4.2 Angular Distribution for Plate 1

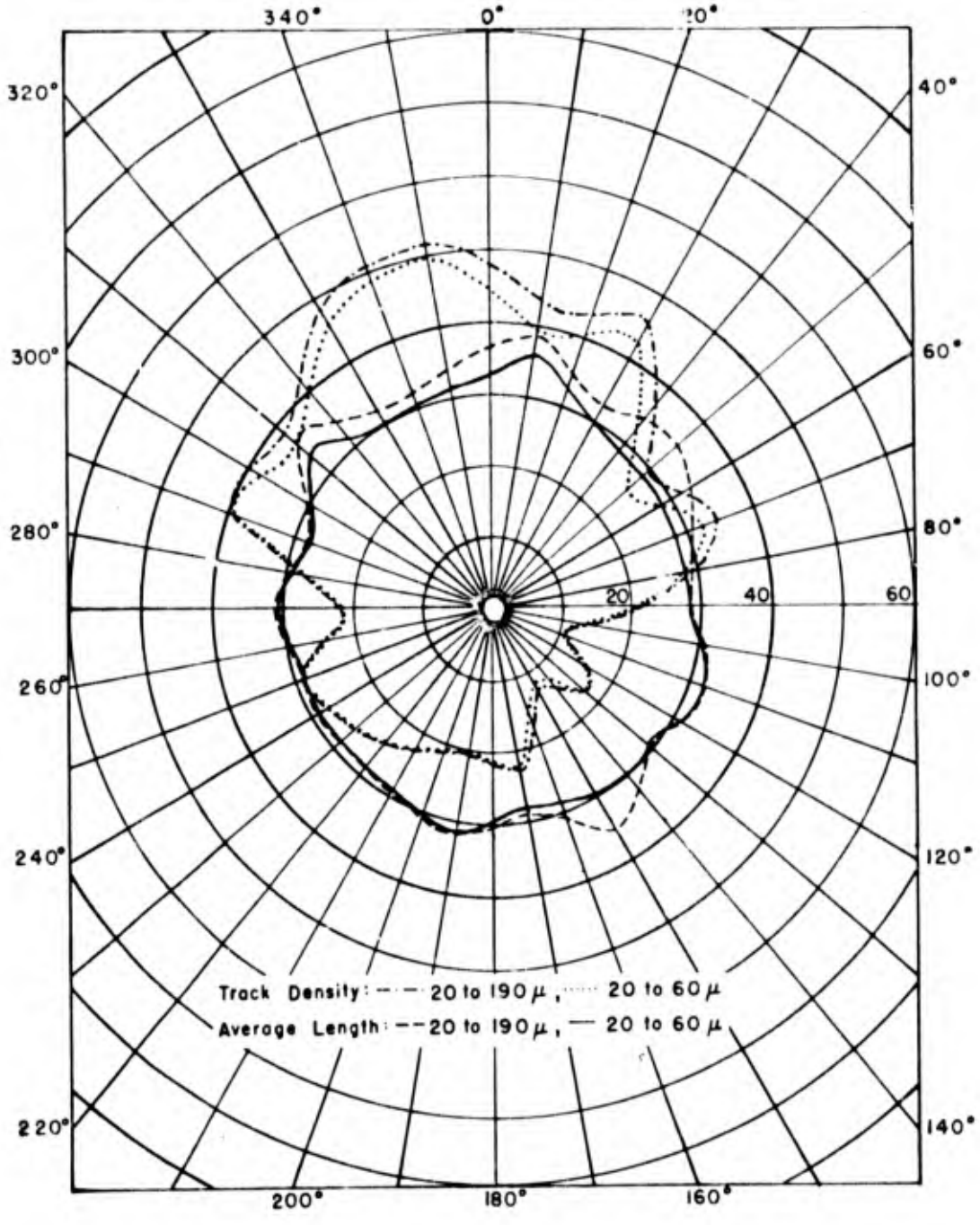

Fig. 4.3 Angular Distribution for Plate 2

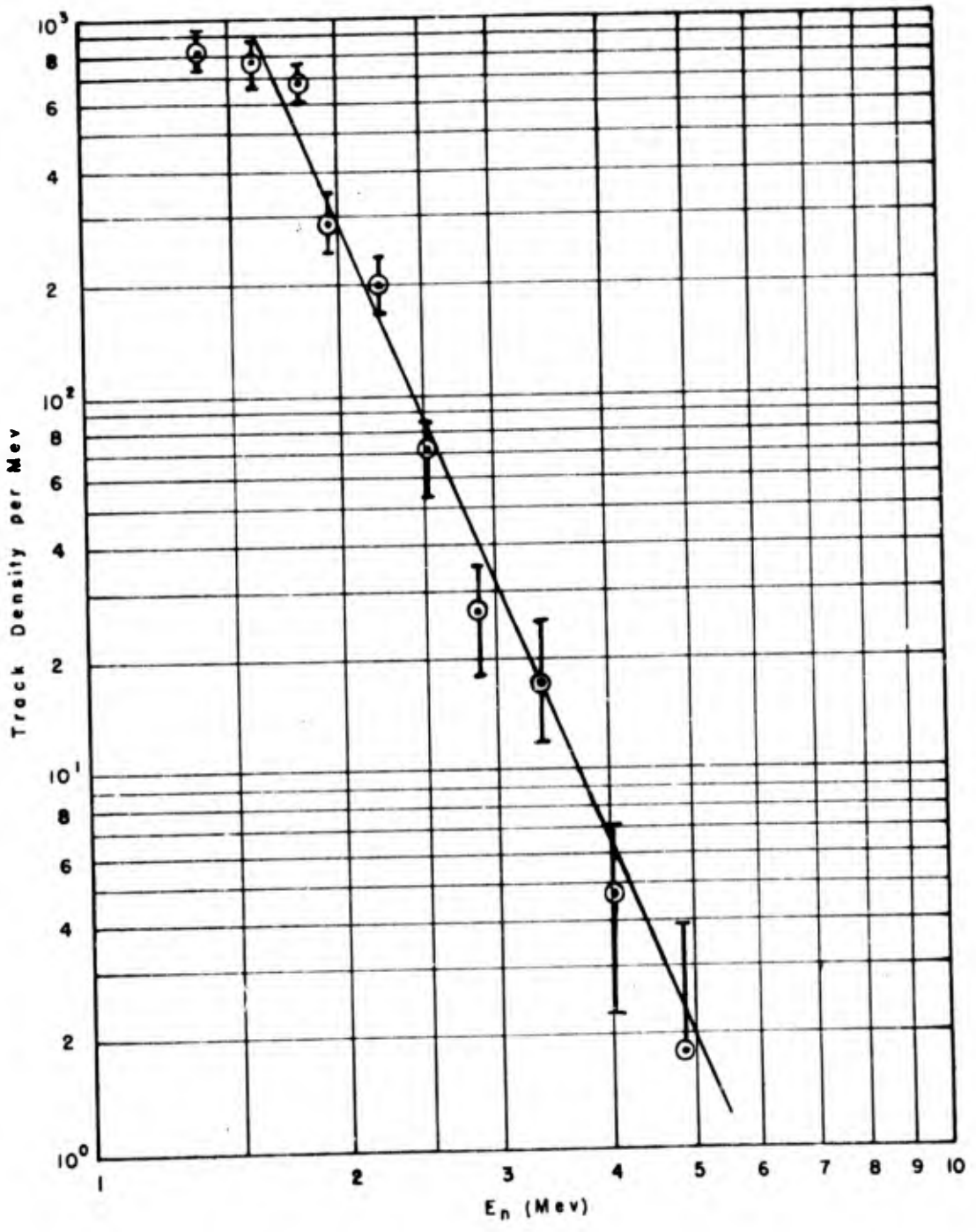

Fig. 4.4 Spectrum Distribution for Plate 1

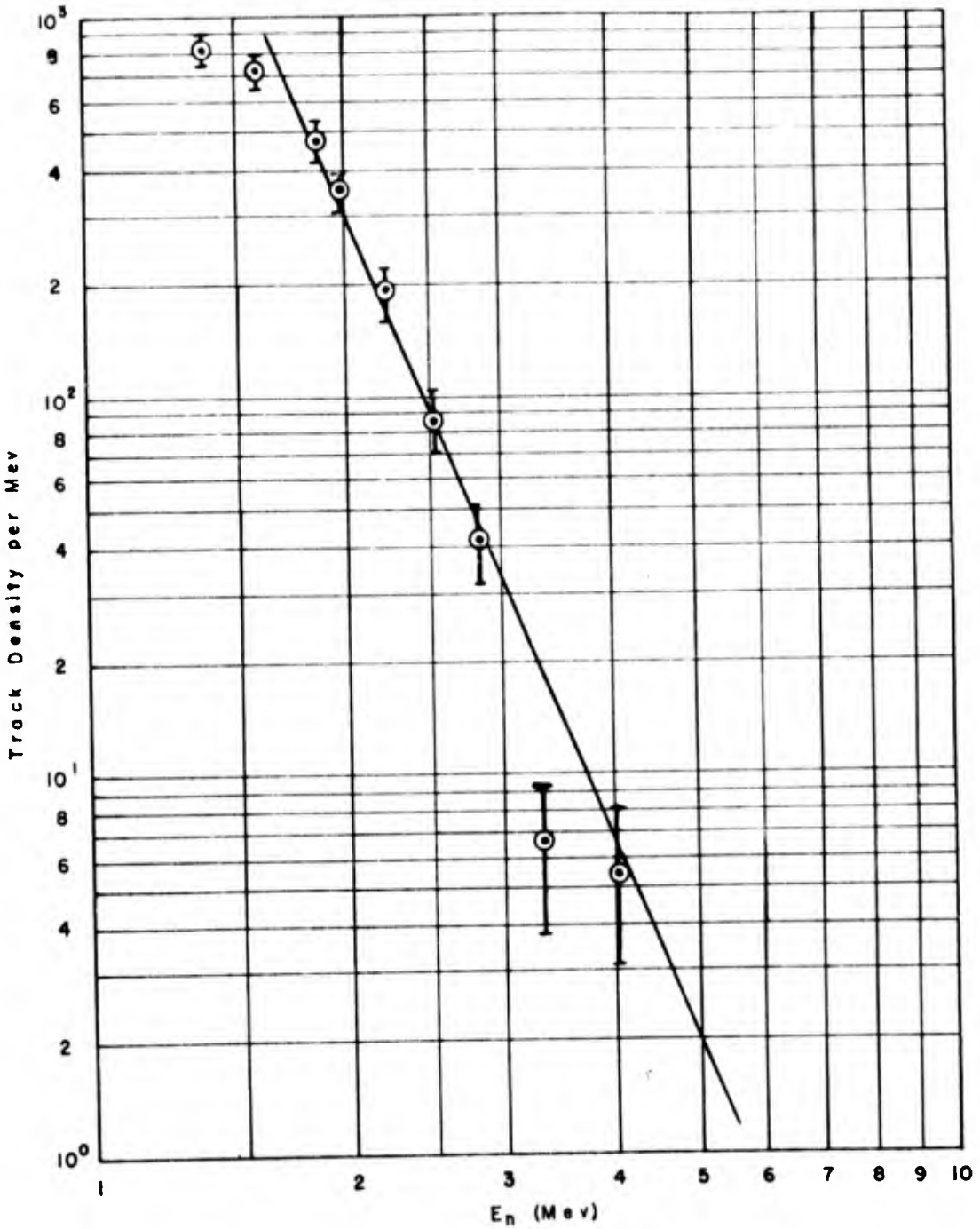

Fig. 4.5 Spectrum Distribution for Plate 2

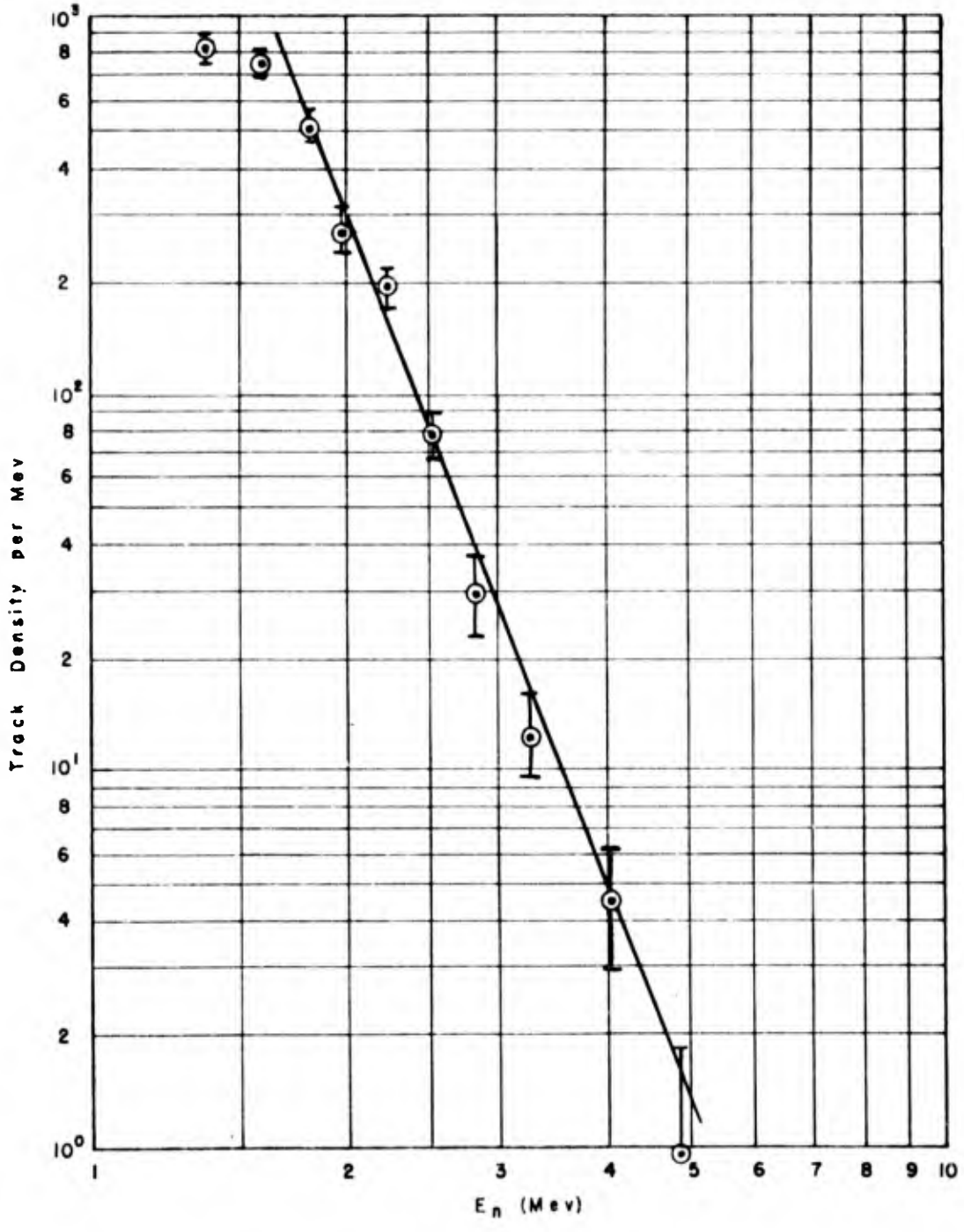

Fig. 4.6 Spectrum Distribution for Plates 1 and 2

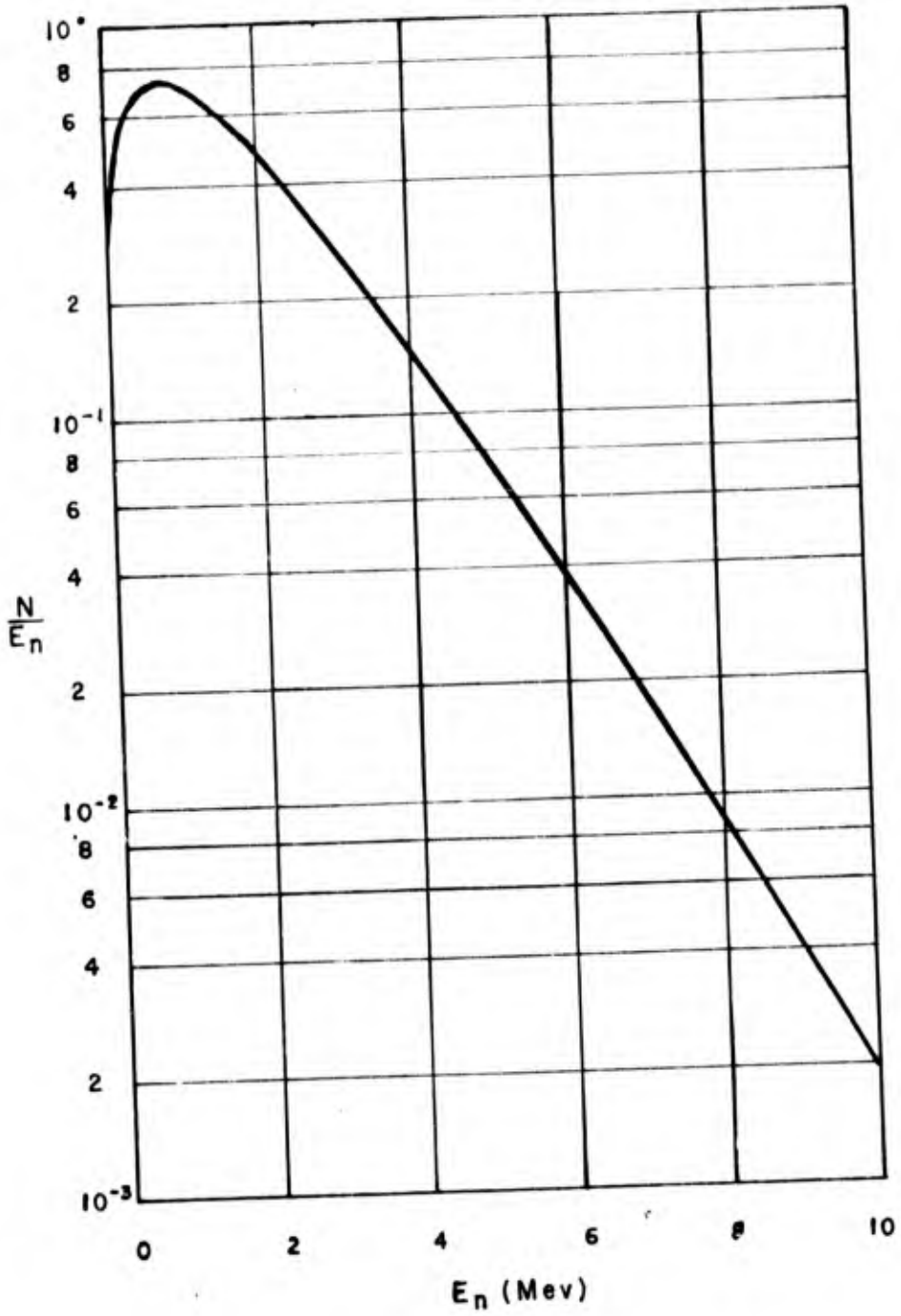

Fig. 4.7 Theoretical Prompt Fission Neutron Energy Spectrum

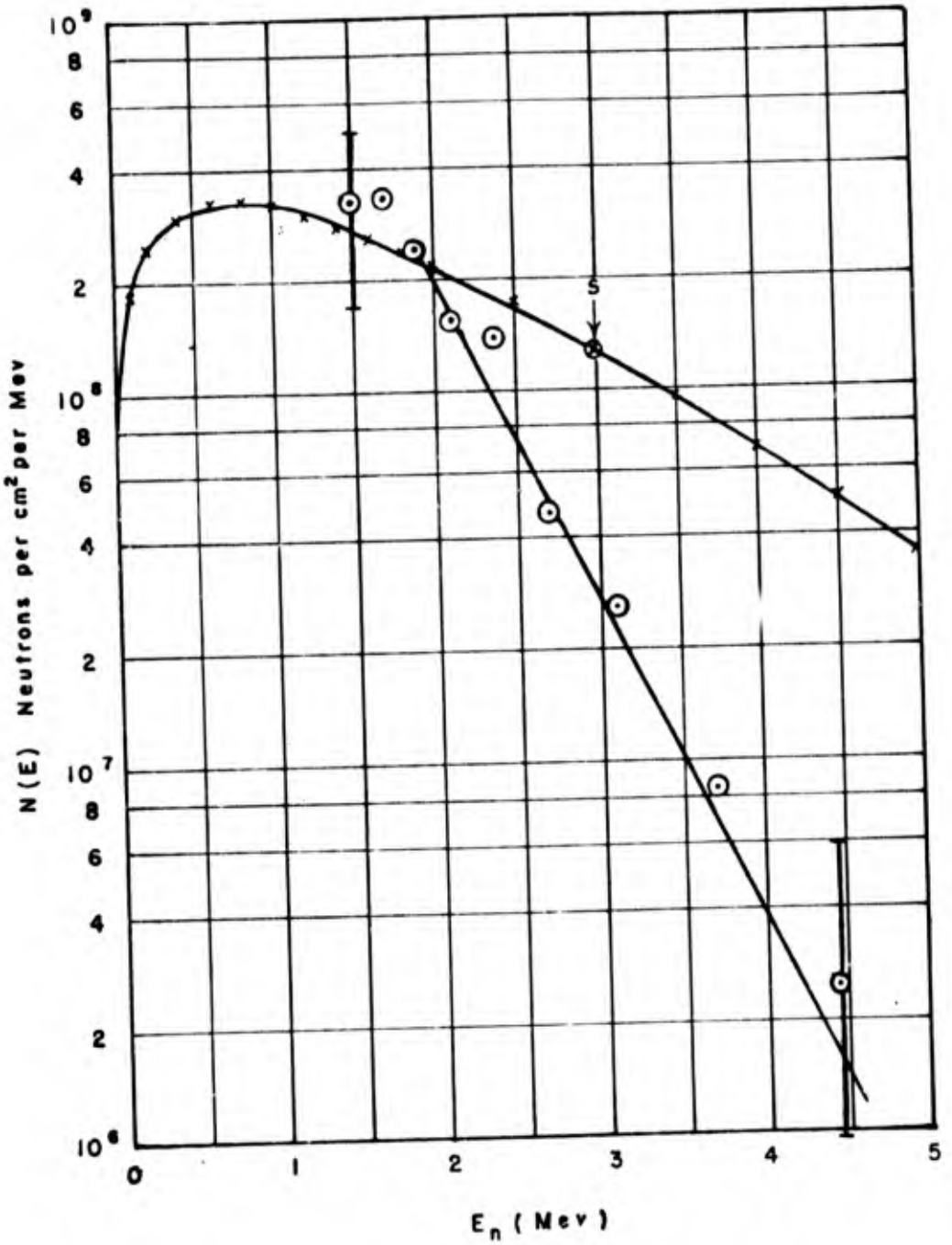

Fig. 4.8 Neutron Energy Spectrum

PART III

CHAPTER 5

FISSION THRESHOLD DETECTORS

5.1 BACKGROUND

Several techniques for neutron detection with fissionable materials have been developed for laboratory use. When fission of a nucleus occurs, the two fission products have kinetic energies of about 100 Mev and ranges equivalent to several mg/cm^2 of absorber. The fission products are unstable and give rise to artificial radioactive series, having an activity whose apparent half life increases with time. In the laboratory, the fission products can be detected directly using ionization chambers, cloud chambers, or nuclear emulsions, or the activity resulting from fission can be measured and the integrated activity or the activity at an arbitrary time gives a measure of the number of fissions. Various difficulties were evident in field application, but on the basis of limited laboratory tests three methods were tested in the field.

5.1.1 Catcher Method

Thin foils of fissionable material were exposed in contact with inert foils; some of the fission products were caught by the inert foils, whose activity could then be measured. A variation of this method was used by LASL to study neutron flux versus time in previous tests, and we learned that they intended to extend this to measurements of integrated flux versus range. This method was adopted to facilitate intercomparison of our data with any obtained by LASL.

The principal disadvantage for our purpose was low sensitivity; fission fragments could be collected from a depth of only a few mg/cm^2, resulting in low activity. This activity decreases rapidly with time, so that sensitivity depends critically on rapid recovery and counting of samples. Also, neutron capture by the catcher foil resulted in an interfering activity which had to be separately measured and corrected.

5.1.2 Foil Method

Foils of fissionable material several mils thick were exposed without catchers and their activity measured. The activity due to fission fragments was greatly increased, but there was a considerable

natural radioactivity and a large activity induced by neutron capture. This method was tried with U^{238} and Th^{232}. Neutron capture in U^{238} produces U^{239}, which decays with a 23.5 min. half life to Np^{239}; Np^{239} decays by beta emission with a 2.33 day half life to Pu^{239}, whose half life is 2.4×10^4 yrs. Six hours after the fission event, the 23.5 min. activity is negligible, and the measured activity is a combination of the fission activity, the 2.3 day Np^{239} activity, and the essentially constant activity of U^{238} (half life 4.5×10^9 yrs.). The thermal capture cross section of U^{238} is 2.8 barns, comparable to the fast fission cross section of about 1/2 barn, so that the fission activity should be detectable the first day after exposure.

Thorium 232 (half life 1.39×10^{10} yrs.) gives rise to the 23.5 min. Th^{233} on neutron capture; the latter decays to Pa^{233} which has a 27.4 day beta activity resulting in U^{233} (half life 1.6×10^5 yrs.). The capture cross section for Th^{232} is higher (7.7 barns for thermals) and its fission cross section lower, but the 27.4 day activity of Pa^{233} should be more easily corrected.

5.1.3 Nuclear Emulsion Method

Thin foils of fissionable material were placed very close to special nuclear emulsions which were very insensitive to gamma rays, electrons, and protons. For fissionable foils less than 1 mg/cm^2 thick, nearly all the fissions gave one product which was recorded in the nuclear emulsion. The sensitivity of this method was quite high. Among the difficulties were the alpha-track background from the natural radioactivity and the fogging produced by intense gamma radiation.

All methods have some of the same inherent difficulties. All fissionable isotopes have measurable fission cross sections for thermal neutrons, which may be due to traces of impurities. Also, gamma rays above about 5 Mev can induce fission, and it is known that there are gamma rays of energies from 5 to 11 Mev present in the radiation from atomic explosions. Most of these gamma rays arise from capture of thermal neutrons by N^{14} in the air. Each method necessarily involved techniques to distinguish photo fission and thermal neutron fission from the fast neutron fission.

5.1.4 Energy Response of Fission Detectors

Four isotopes appeared suitable for our measurements. Uranium 238 and Th^{232} have thresholds for neutron fission near 1 Mev, and Np^{237} and Pa^{231} have thresholds below 0.5 Mev. The expected relative response of these as a function of neutron energy is compared to that of $S^{32}(n,p)$ in Fig. 5.1. These curves were obtained by multiplying the fission cross sections by the relative number of neutrons at each energy in the fast reactor at LASL, extrapolating an experimentally determined distribution function to zero energy. This should

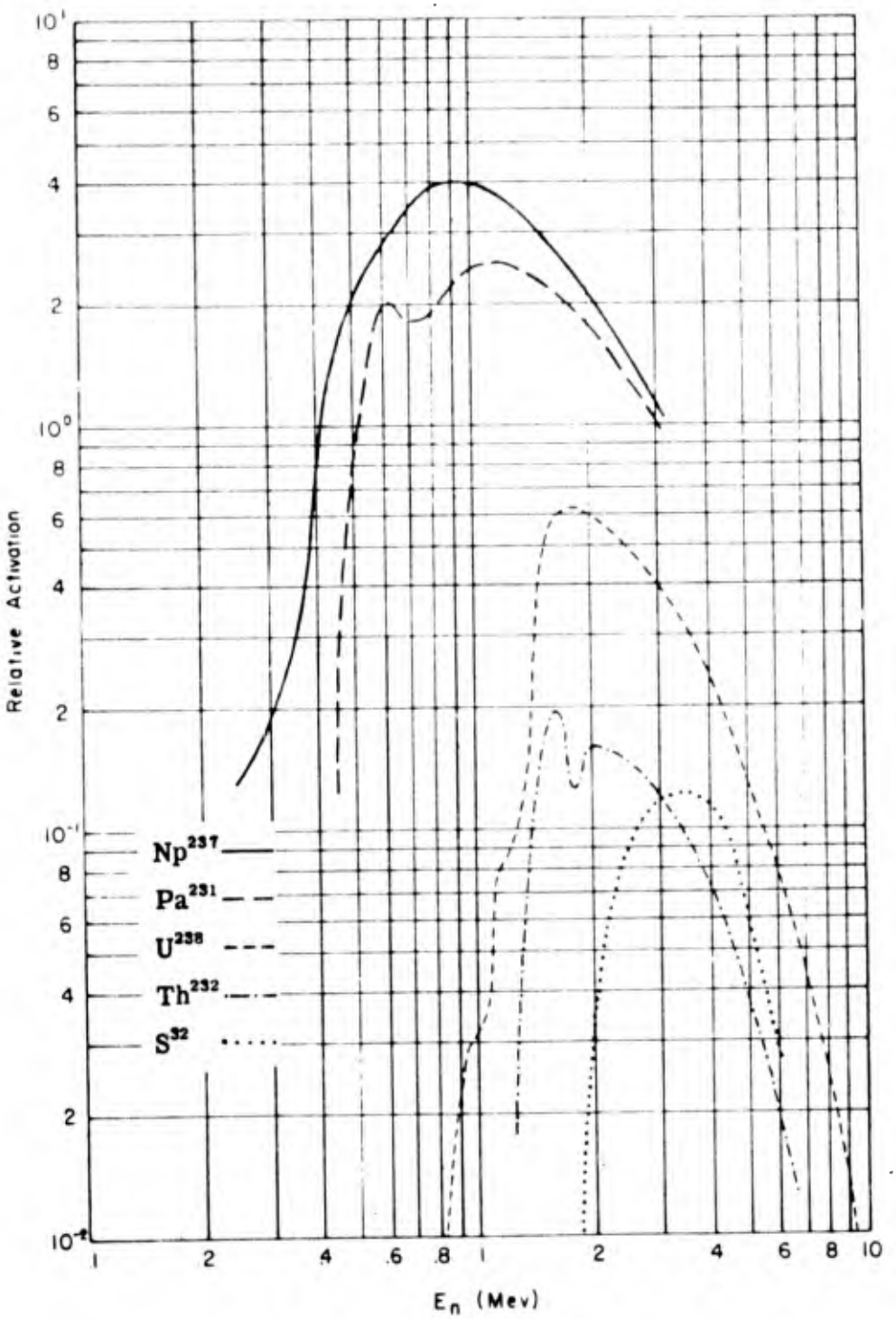

Fig. 5.1 Relative Response of Fission Detectors and Sulphur to Moderated Fast Neutron Fission Flux

approximate closely the relative response of each detector to the flux from an ordinary fission-type atomic device. Above 1 Mev, the experimental curve used agrees well with the theoretical expression $e^{-E} \sinh (2E)^{\frac{1}{2}}$ for energy dependence of fission neutrons and the extrapolated value for thermal neutrons gives the correct ratio for thermal flux to sulphur-neutron flux.

The ordinates of the curves at 2.6 Mev give the actual cross sections in barns at this energy.

Of the four isotopes, only Th^{232} was readily obtainable with high purity. Ordinary uranium contains 0.714 per cent U^{235}, which has a fission cross section for thermal neutrons roughly 1000 times that of U^{238} for fast neutrons. Protoactinium 231 is extremely rare, being obtained from the natural decay of U^{235}. Neptunium 237 is artificially produced in reactors, and the amounts are quite small.

5.2 INSTRUMENTATION

5.2.1 Catcher Method

Sandwiches were made with 1 mil CP aluminum foil between two pieces of uranium or thorium foils a few mils thick. It was intended to use circular foils 1" in diameter, but material limitations necessitated the use of 1/2" diameter foils. These were generally placed in the gold-type holders described in Part I for exposure. One sandwich in a holder was bare, and another enclosed in a 0.40" thick cadmium shield, to observe the thermal neutron effect. Another piece of 1 mil Al foil was placed outside the Cd shield to measure the induced activity in the Al catcher.

The holders were exposed without lead shielding, inside a 1 1/2" thick lead sphere, inside a 3" thick lead sphere, and inside the 7" thick lead hemispheres used in Project 4.3.

5.2.2 Foil Method

Some of the uranium and thorium foils used in the catcher method were counted after exposure. In addition, some single foils were exposed, with and without Cd shielding, in the same type holders, for Shot 8. Los Alamos Scientific Laboratory furnished some depleted uranium foils 3 1/2 mils thick; ordinary uranium foils ranged from 3 1/2 mils to 1 mil in thickness. Thorium foils were 7 mils thick.

5.2.3 Nuclear Emulsion Method

Eastman Kodak nuclear plates, type NTC, 1" x 3", were used to record the fission fragments. Thin films of fissionable material were painted or electroplated onto thin platinum dishes 1" or 3/4" in

diameter. A row of three or four foils was placed in a 10-mil aluminum box with a 5 mil Teflon spacer separating them from the nuclear emulsion. These cassettes were exposed in pairs, one pair having a 40-mil Cd shield around it. The complete cassette was usually placed in a rectangular steel holder with 1/4" thick walls, although a holder with 1/8" thick aluminum walls was also tried. Rectangular lead shields of 1" and of 2" wall thickness were used. The foils were placed so that the nuclear emulsion faced the atomic device in the field.

Several other types of emulsions were also tested but found unsatisfactory. Some emulsions were loaded with natural uranium or thorium salts to test the feasibility of this technique.

5.3 OPERATIONS

Measurements were seriously hampered by lack of suitable detectors. For Shot 4, 16 depleted uranium foils were loaned by LASL and were used to instrument the George station of Project 4.3. Pairs of these were used in the catcher method with and without Cd shielding to study the neutron attenuation in lead. This was supplemented by studies of gold and sulphur in lead shields. The nuclear emulsion technique was tested in the field during Shot 4, but no flux data could be obtained since natural uranium was used.

For Shot 8, 20 thorium foils 1/2" in diameter and five 1" in diameter were available, in addition to 15 of the LASL depleted uranium foils and 15 natural uranium foils. Also available were three foils of Pa^{231} about 0.1 mg/cm^2 thick, and four of Np^{237} of about the same thickness. There was not enough Np^{237} or Pa^{231} to use in the catcher or foil methods at the Project 4.3 stations, so they were used in the nuclear emulsion method although their high natural activity made this of questionable value. Natural uranium oxide and thoria films were used with the Np and Pa.

Since preliminary data from Shot 4 indicated the feasibility of the foil method, it was decided to concentrate on this in an effort to obtain data from more stations. Depleted and natural uranium foils were used in the catcher technique outside the Project 4.3 Easy station to measure the effect of the U^{235} impurity in the depleted uranium. The catcher technique was also used with depleted uranium and with thorium at the 300-yard station to intercalibrate these detectors. The foil method was also used at the 300-yard station for intercalibration purposes. The higher flux at this station would give more accuracy in intercalibration and facilitate use of LASL data on photo-fission and good geometry neutron spectra in interpretation of data. The remainder of the thorium foils were used to instrument other Project 4.3 stations.

After recovery of the samples from the field, the Al catchers and blanks and the foils were counted with the pre-flush flow counter

described in Part I. Both sides of the foils were counted, and Al absorber data were obtained to investigate maximum efficiency. The Al catchers were counted on the top side only, since both sides gave nearly the same activity. At least three sets of counts were made on each sample over a period of several days. The fission foils were counted until the half life associated with neutron capture could be identified, and the activity of selected foils were followed for several half lives.

The nuclear emulsion plates were developed as soon as feasible using standard techniques. Simultaneously unexposed plates and plates which had been exposed to the foils (but no neutrons) were developed.

5.4 RESULTS

A summary of the data which could be used to calculate integrated neutron fluxes is given in Table 5.1. The U^{238} counting rates are accurate to 10 per cent, and those for Th^{232} to 50 per cent. The measured activities of catchers and foils were corrected for counting rate losses where necessary and then corrected for variations in counter sensitivity as determined by counting rates of secondary standards. These counting rates were corrected for induced activity in the catchers or natural radioactivity of the foils. For the foils, the induced activity was determined by plotting the corrected activities and extrapolating the residual induced activity to zero time; appropriate corrections for induced activity then gave the activity due to fission in these foils.

A standard decay curve for fission fragments was constructed using data taken in the laboratory on activity versus time for fission fragments formed in betatron irradiation and reactor exposure of natural uranium. The best straight line was drawn through the region of interest of a logarithmic plot, choosing 36 hours after bombardment as the arbitrary time for comparison. The final corrected data for each catcher and foil were plotted on this graph, and the standard curve was used to give the best interpolation (or extrapolation, unfortunately) of this data to the 36-hour time. It is this activity at 36 hours which is taken as a measure of the total fission yield, and is given in Table 5.1.

The total gamma ray intensity in the 7" lead hemispheres was 5 roentgens or less, so photo-fission was negligible here. The energy response of U^{238}, Th^{232}, and $S^{32}(n,p)$ is sufficiently similar to allow the assumption of similar neutron attenuation. Thus we concluded that photo-fission was negligible at the Project 4.3 stations.

TABLE 5.1

Shot 4

Detector	Type	Slant Distance (yards)	Shielding		Activity at 36 hr. (cpm)	Corrected Activity (cpm)	Total Flux (n/cm^2)
			Cadmium	Lead			
Al #1	U^{238}	1027	0.040"	0	95	88	2.7×10^{11}
Al #2	U^{238}	1027	0	0	138		
Al #7	U^{238}	1027	0	1½"	119		
Al #9	U^{238}	1027	0.040"	1½"	73	66	2.0×10^{11}
Al #10	U^{238}	1027	0	3"	108		
Al #12	U^{238}	1027	0.040"	3"	64	57	1.7×10^{11}
Al #5	U^{238}	1027	0	7"	62		
Al #4	U^{238}	1027	0.040"	7"	27	21	6.6×10^{10}
Shot 8							
Al 28-12	U^{238}	1105	0	0	36.0		
Al 28-10	U^{238}	1105	0.040"	0	18.0	15.0	4.5×10^{10}
Al U-6	Natural Uranium	1105	0	0	377		
Al U-5	Natural Uranium	1105	0.040"	0	78.0		
Al 28-14	U^{238}	316	0.040"	0	5820	4850	1.4×10^{13}
Al T-14	Th^{232}	316	0	0	1600		
Al T-12	Th^{232}	316	0.040"	0	760		
Al T-31*	Th^{232}	316	0	0	2900		
Al T-33*	Th^{232}	316	0.040"	0	1900		

* These detectors were 1" in diameter, rather than ½".

The data from shot 8 were used to determine the correction for the residual U^{235} in the depleted uranium samples. The cadmium difference of 299 cpm for catchers Al U-6 and Al U-5 was due predominantly to the 0.714 per cent U^{235} present in the natural uranium, giving a counting rate of 4.19 cpm for each 0.01 per cent U^{235}. The cadmium difference of 18.0 cpm for the depleted uranium catchers Al 28-12 and Al 28-10 was thus computed to indicate the presence of 0.043 per cent of U^{235}. This is in adequate agreement with the value 0.034 per cent obtained from mass spectrographic analysis at Oak Ridge National Laboratory; the net counting rate for Al 28-10 is about half the background due to cosmic rays.

The difference in counting rates for the Cd shielded samples Al 28-10 and Al U-5 of 60.0 cpm indicated a significant epithermal contribution from U^{235}. This amounted to 3.0 cpm for the catcher Al 28-10, giving a net counting rate at 36 hours of 15.0 cpm due to fission of U^{238} by fast neutrons. The ratio of epithermal effect to thermal effect was 3.0/18.0 = 0.167. This ratio was used to correct the counting rates of the other Cd shielded samples of depleted uranium.

To estimate the integrated flux detected by the depleted uranium catchers, the ratio of the net counting rate for Al 28-10 was compared to the cadmium difference for Al U-6 and Al U-5, using the known percentage of 0.714 per cent U^{235} in the latter and the integrated flux of 9.16×10^{10} n/cm^2 measured with gold detectors at this range. Taking the thermal fission cross section of U^{235} as 549 barns and using the value 0.40 barns at 1.9 Mev for U^{238}, the integrated flux for the U^{238} catcher was 4.5×10^{10} n/cm^2. The calibration factor was computed to be 3.1×10^9 n/cm^2/cpm. The neutron intensities calculated from this calibration number are estimated to be within a factor of 2 of the correct value, and are probably a bit high. The average cross sections for U^{235} and for U^{238} are both lower than those taken.

The calibration factor computed above is checked adequately by some early work done at LASL. Using a depleted uranium sample 2" x 1/2" with a cellophane catcher, exposing to a known flux of 14 Mev neutrons and counting with a thin glass walled Geiger counter, a calibration number of 6.4×10^8 n/cm^2/cpm was obtained. Correcting this number for area of detector gives a calibration number of 3.3×10^9 n/cm^2/cpm, which should be reduced by a factor of about 2 to compensate for absorption.

Sample Al 28-1 was counted at LASL to permit a more accurate calibration if one is made there. A 36-hour counting rate of 95 cpm under our standard conditions is to be compared to a counting rate of 134 cpm computed from data on their counter No. 3 which had a counting rate of 44,640 cpm with their standard No. 4 at 01:30 MDST May 3, 1952, when the data were taken.

It is possible that an appreciable photo-fission correction is required for the data from Shot 8, although this is not likely at the George station. A calculation of this effect requires knowledge of the yield of high energy gamma rays which is not available at present.

Unfortunately, recovery of samples at the 300-yard station of Shot 8 was delayed 60 hours. By this time the catcher activities were quite weak (1/10 of that 8 hours after irradiation), and a large extrapolation was required to the 36-hour point.

The Th^{232} catcher data had an inexplicably large scatter, and counting rates for it are not reliable to better than 25 per cent. The cadmium ratio was about a factor of 2, which seems too large. The thermal fission cross section for Th^{232} is less than 0.2 mb, and the uranium contamination of our samples was given as about 1 part per million. The cause of the large cadmium difference must be determined before an accurate correction can be made. The ratio of counting rates for Th^{232} catchers and U^{238} catchers is 1:8, somewhat less than would be expected from cross section considerations, but within reason when thresholds are considered. The data obtained are not considered sufficiently accurate to warrant calculation of a calibration number for Th catchers.

No fluxes were calculated from the foil method. The intercalibration foils at the 300-yard station were not recovered until 60 hours had elapsed. Essentially one counting rate was measured for Th foil before the field station was dismantled, and this was the only point which gave a significant net activity; all the activities measured in Washington, D. C. were due to the combination of natural radioactivity and the 27.4 day activity of Pa^{233}. The uranium foils were useless. The Th foils inside the Project 4.3 stations were recovered rapidly, but there was insufficient flux to estimate its quantity. The total activity due to fission and capture was only about 10 per cent of the natural radioactivity 6 hours after exposure, and unusual variations of several per cent in counter efficiency over a period of a few hours helped make it impossible to satisfactorily distinguish fission activity and induced activity.

No data were obtained with Np or Pa due to excessive fogging of the nuclear emulsions by natural and induced radioactivity. The uranium and thorium films demonstrated the superior sensitivity of this method, but contaminants precluded their use for fast neutron flux measurements.

The integrated fluxes as a function of lead thickness for Shot 4 are shown in Fig. 5.2. The sulphur data from Shot 8 are included for comparison. Thermal neutrons were attenuated only slightly by 7" of lead; the attenuation of fast neutrons is greater, but is similar for those detected by U^{238} and by $S^{32}(n,p)$. The points at 7" of lead are

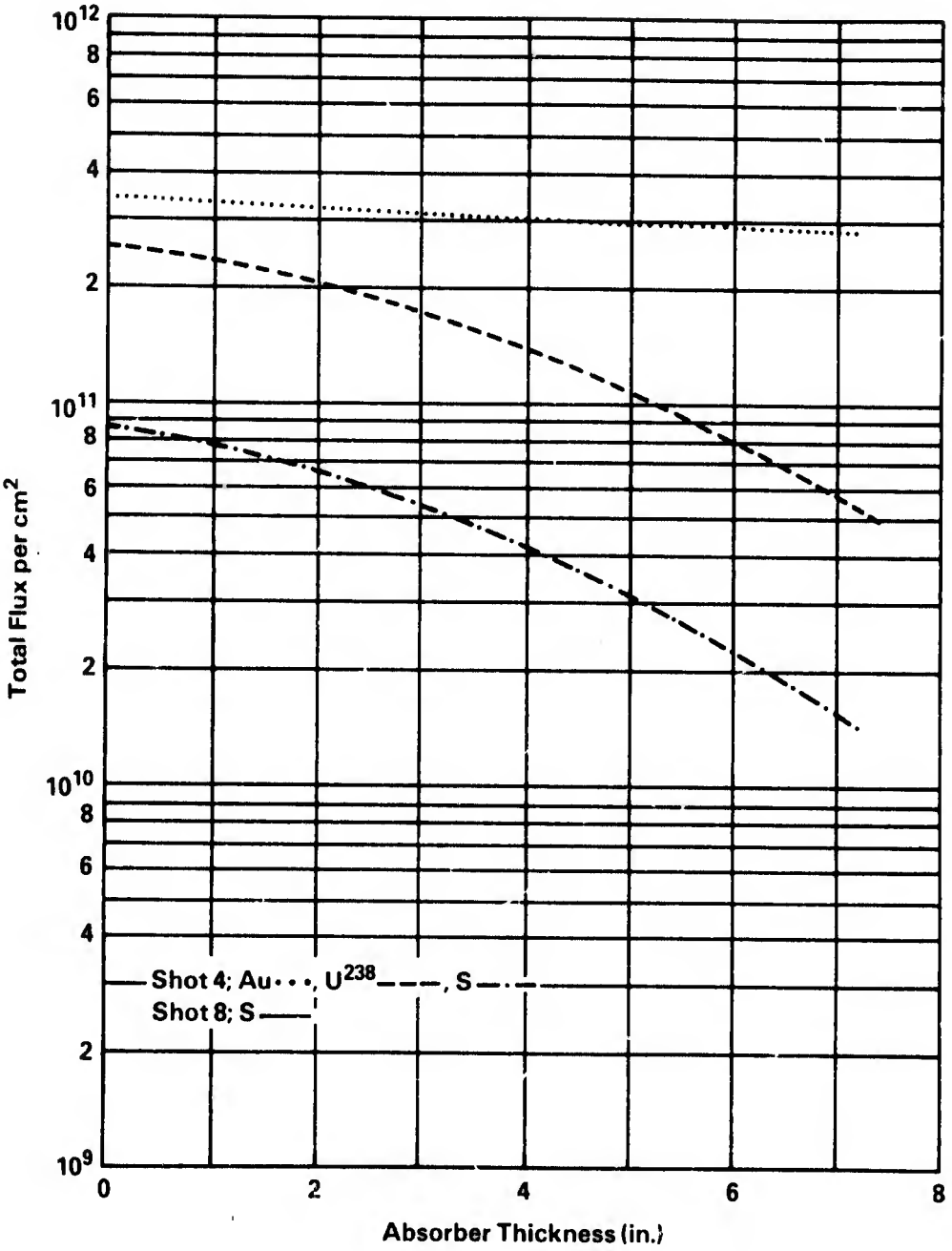

Figure 5.2 Neutron Attenuation in Lead.

least reliable, because of the low activities, the different design of the lead, and the placement of the samples.

To facilitate comparison of the attenuation of fast neutrons in lead, normalized data are presented on a linear plot in Fig. 5.3. The data for U^{238} from Shot 4 have been divided by 3, and that for sulphur in Shot 8 have been multiplied by 10. Within experimental error, the attenuation is linear and of the same magnitude for all three cases. There is some indication that the attenuation is greater for Shot 8 than Shot 4, and that it is less (and possibly exponential) for U^{238} than S^{32}. [redacted] and the degradation of neutron energy by the lead, make this plausible, but the data are not sufficiently accurate to conclude this definitely.

The ratio of U^{238} neutrons to sulphur-neutrons at the Project 4.3 installation was approximately [redacted]

[redacted] Shot 8 had a considerably larger ratio of gamma radiation to fast neutron flux than Shot 4, so it is possible that photo-fission had contributed appreciably to the values quoted for U^{238} neutrons in Shot 8. The ratio expected for the two groups of neutrons in Shot 8 is approximately 3 if the fast neutron spectrum is similar to a fission neutron spectrum, [redacted] It is believed that the observed ratio is more likely to be somewhat high than that there is a radical departure from the expected spectrum.

5.5 CONCLUSIONS

Both the catcher method and the nuclear emulsion method are feasible (within limitations of neutron and gamma ray intensities) using U^{238} and Th^{232}. The catcher method is superior for high neutron fluxes, and the nuclear emulsion method excels for low neutron fluxes. The catcher method will work for Np^{237} and Pa^{231} if sufficient quantities of these can be obtained. The nuclear emulsion method would work well with them if their exposure to the emulsion could be reduced to the order of minutes. The foil method may be successful with Th^{232} at intermediate fluxes, but seems to have little advantage over the catcher method. Any method relying on the activity of the fission fragments requires prompt recovery and counting of samples for accuracy.

Uranium 238 is superior to Th^{232} in energy response and sensitivity, even when 0.05 per cent U^{235} is present. Higher depletions of uranium would greatly simplify the taking of data and its analysis. The only advantage of Th^{232} seems to be its availability. Neptunium 237 is slightly superior to Pa^{231} and is somewhat more plentiful.

Loading nuclear emulsions with Th^{232} or U^{238} salts is feasible but not desirable for measuring neutron fluxes.

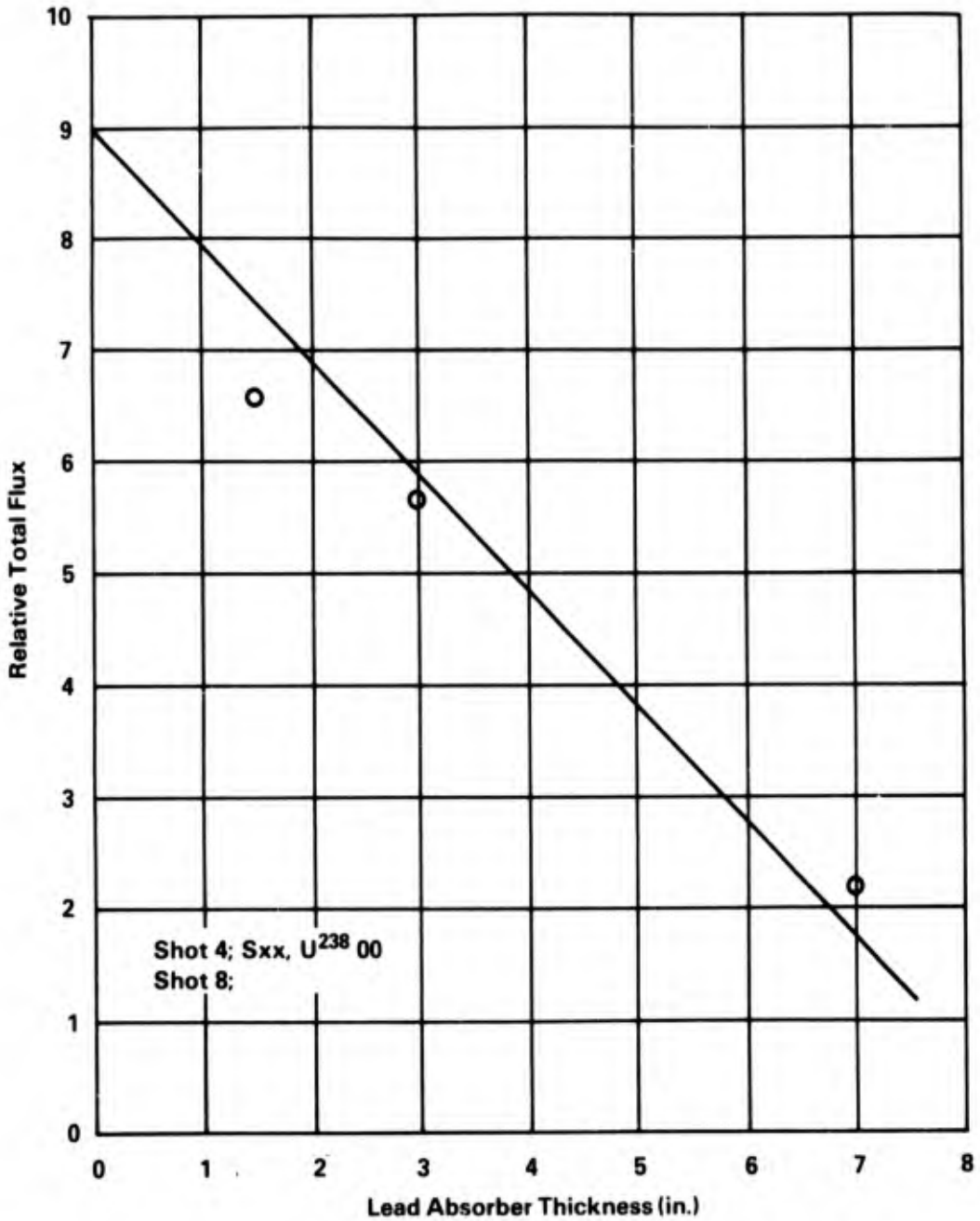

Figure 5.3 Relative Fast Neutron Attenuation.

Uranium^{238} and Th^{232} have approximately the same energy response to neutrons from the explosion of an atomic device, and detect [illegible] times the number measured by the $S^{32}(n,p)$ reaction. Attenuation of the fast neutrons in lead appears to be more nearly linear than exponential.

5.6 RECOMMENDATIONS

A calibration should be made for the U^{238} catcher method.

Further work could profitably be done on Th^{232} as a neutron detector, since it is available in quantities which permit techniques too wasteful for the other isotopes. Perhaps a study of optimum foil thickness and absorber thickness would give considerable improvement in the foil method. Since the capture cross section of Th^{232} averages more than 10 times the fission cross section, this approach is not the most promising.

Any further work with the nuclear emulsion method should involve a simple device to expose the radioactive films to the emulsion only during the neutron irradiation. This will increase the ultimate sensitivity by reducing enormously the alpha-particle background and make plate reading much easier with the reducing fogging. It is easier (and more accurate with inexperienced personnel) to count both alpha particles and fission fragments, and correct for alpha particles with a control exposure, than it is to count only fission fragments. For measurement of neutron flux versus range, a series of fissionably films of graded thicknesses is desirable. The effective thickness can more easily be obtained from alpha counting than from weighing.

Attention should be given Li^6 loaded nuclear emulsions from neutron spectra measurements inside lead shields such as those used in Project 4.3 which reduce gamma dosage below 5 roentgens. A preliminary trial was made using some old emulsions available, but these proved to be fogged by age.